

UNIVERSIDADE
DE SANTIAGO DE COMPOSTELA

Facultade de Química

Abiotic reactions promoted
by the cell machinery
PART A



GRAO EN QUÍMICA

Curso 2022/23

Alumno/a: David Montoto Pintos



FACULTADE DE QUÍMICA

José Luis Mascareñas Cid, titor e docente do Departamento de Química Orgánica, e María Tomás Gamasa, cotitora e docente do Departamento de Química Orgánica, autorizan a presentación do Traballo de Fin de Grao do alumno David Montoto Pintos na convocatoria de xullo do curso 2022-2023, o cal foi realizado baixo a súa dirección no Centro Singular de Investigación en Química Biolóxica e Materiais Moleculares da Universidade de Santiago de Compostela (CiQUS).

E para que así conste asinamos o presente informe en Santiago de Compostela o 3 de xullo de 2023.

Abbreviations

ADP	adenosine diphosphate	NAD ⁺	nicotinamide adenine dinucleotide (oxidized form)
ATRP	atom transfer radical polymerization	NADH	nicotinamide adenine dinucleotide (reduced form)
BNAH	N-benzyl-1,4- dihyronicotinamide	NAD(P)H	nicotinamide adenine dinucleotide or dinucleotide phosphate (reduced form)
CuAAC	copper-promoted azide-alkyne cycloaddition	NMR	nuclear magnetic resonance
d	doublet	PBS	phosphate-buffered saline
DMEM	Dulbecco's modified Eagle's medium	ppm	parts per million
DMSO	dimethyl sulfoxide	RAFT	reversible addition- fragmentation chain transfer
<i>E. coli</i>	<i>Escherichia coli</i>	ROS	reactive oxygen species
e.g.	<i>exempli gratia</i>	r.t.	room temperature (approximately 21 °C)
EET	extracellular electron transfer	Ru(bpy) ₃	tris(bipyridine)ruthenium(II) hexafluorophosphate
ETC	electron transport chain	ρ	density
eq.	equivalents	s	singulet
EWG	electron withdrawing group	<i>S. cerevisiae</i>	<i>Saccharomyces cerevisiae</i>
EY	eosin Y	SET	single electron transfer
FBS	fetal bovine serum	SPAAC	strain-promoted azide-alkyne cycloaddition
g	relative centrifugal force	TEMPO	(2,2,6,6-tetramethylpiperidin- 1-yl)oxyl
GSH	L-glutathione	THF	tetrahydrofuran
GSSG	glutathione disulfide	UV	ultraviolet
¹ H-NMR	proton NMR	v/v	volume/volume
HS	heat shock		
IED-DA	inverse electron-demand Diels-Alder reaction		
IR	infrared		
<i>L. lactis</i>	<i>Lactococcus lactis</i>		
LB	Lysogeny broth		
m	multiplet		
MW	molecular weight		
NaAsc	sodium ascorbate		

Table of contents

Abstract	6
1. Introduction	8
1.1. Bioorthogonal chemistry	8
1.2. Biocompatible chemistry	9
1.2.1. Definition and applications of biocompatible chemistry.....	9
1.2.2. Reactions promoted by cellular redox processes.....	10
1.2.3. Reactions promoted by abiotic catalysts	12
1.2.4. Future projection of abiotic biocompatible chemistry.....	12
1.3. Chemistry of arenediazonium salts	13
1.3.1. General reactivity of arenediazonium salts	13
1.3.2. The Meerwein arylation	14
2. Objectives and work plan	14
2.1. Objectives	14
2.2. Work plan	15
3. Results	15
3.1. (Non-)Photocatalyzed reactions in cells: a frustrating finding.....	15
3.2. Evaluation of the photocatalyzed reaction	16
3.3. <i>In vitro</i> experiments.....	18
3.3.1. Screening of different biological reductants.....	18
3.3.2. Optimization of conditions and study of the NADH-promoted reaction ...	20
3.3.3. Evaluation of alternative acceptors	25
3.3.4. Reactions with alkynes	25
3.4. Experiments in cells	26
3.4.1. ATP viability assay	26
3.4.2. Evaluation of the reaction in HeLa cells	27
3.4.3. Cell fractionation experiments	28
3.4.4. Experiments in <i>E. coli</i>	30
3.5. Experimental procedures	31
3.5.1. General information for <i>in vitro</i> experiments.....	31
3.5.2. Synthesis of p-methoxyphenyldiazonium tetrafluoroborate (1)	32
3.5.3. Synthesis of 2-(4-methoxyphenyl)naphthalene-1,4-dione (2)	32
3.5.4. Synthesis of 2,3-bis(4-methoxyphenyl)naphthalene-1,4-dione (3)	33

3.5.5. Representative procedure for irradiation experiments in subsection 3.2 ...	33
3.5.6. Representative procedure for reactions in subsection 3.3	34
3.5.7. Representative procedure for reactions in subsection 3.3.4	34
3.5.8. Internal standard method for yield quantification	34
3.5.9. General information for cell culture experiments	36
3.5.10. Luminescence viability assay	36
3.5.11. Experiment in HeLa cells	36
3.5.12. Cell fragmentation assay	37
3.5.13. Experiments in <i>E. coli</i>	37
3.5.14. Quantification by HPLC-MS.....	38
4. Conclusions	38
References	40
Annex: NMR spectra.....	49

Abstract

The development of new-to-nature, non-enzymatic biocompatible reactions that interact with the metabolism of living systems represents an emerging field at the interface of chemical synthesis and synthetic biology. These reactions could be used to access novel synthetic routes, and they have potential applications in biomedicine and biology. In this Degree Final Project, we report the discovery of a Meerwein arylation reaction between diazonium salts and naphthoquinone derivatives promoted by living cells. The process has been carried out in mammalian cells (HeLa and A549) and *E. coli*, and it has been found to proceed in isolated mitochondria and mitochondria lysates. Low-weight biological reductants such as NADH, glutathione and ascorbate promote the reaction in abiotic media. Finally, preliminary studies to expand the scope of this transformation to other diazonium salts or other radical acceptor partners have been undertaken, opening the door to interesting structures like benzothiophenes and phenanthrenes.

Resumen

El desarrollo de reacciones biocompatibles no enzimáticas nuevas en la naturaleza que interactúan con el metabolismo de los sistemas vivos representa un campo emergente en la interfase entre la síntesis química y la biología sintética. Estas reacciones podrían utilizarse para acceder a nuevas rutas sintéticas, y tienen aplicaciones potenciales en biomedicina y biología. En este Trabajo de Fin de Grado, se describe el descubrimiento de una reacción de arilación de Meerwein entre sales de diazonio y derivados de la naftoquinona inducida por células vivas. El proceso se ha llevado a cabo en células de mamífero (HeLa y A549) y *E. coli*, y se ha observado que tiene lugar en mitocondrias aisladas y lisados de mitocondrias. Los reductores biológicos de bajo peso molecular como el NADH, el glutatión y el ascorbato favorecen la reacción en medios abióticos. Finalmente, se han llevado a cabo estudios preliminares para ampliar el alcance de esta transformación a otras sales de diazonio u otros sustratos aceptores de radicales, abriendo la puerta a estructuras interesantes como los benzotiofenos y los fenantrenos.

Resumo

O desenvolvemento de reaccións biocompatibles non enzimáticas novas na natureza que interactúan co metabolismo dos sistemas vivos representa un campo

emerxente na interfase entre a síntese química e a bioloxía sintética. Estas reaccións poderían utilizarse para acceder a novas vías sintéticas, e teñen aplicacións potenciais en biomedicina e bioloxía. Neste Traballo de Fin de Grao, descríbese o descubrimento dunha reacción de arilación de Meerwein entre sales de diazonio e derivados da naftoquinona inducida por células vivas. O proceso levouse a cabo en células de mamífero (HeLa e A549) e *E. coli*, e observouse que ten lugar en mitocondrias illadas e lisados de mitocondrias. Os redutores biolóxicos de baixo peso molecular coma o NADH, o glutatión e o ascorbato favorecen a reacción en medios abióticos. Finalmente, realizáronse estudos preliminares para ampliar o alcance desta transformación a outras sales de diazonio ou outros substratos aceptores de radicais, abrindo a porta a estruturas interesantes coma os benzotiofenos e os fenantrenos.

1. Introduction

1.1. Bioorthogonal chemistry

The concept of bioorthogonal chemistry was introduced at the beginning of the 21st century by Carolyn R. Bertozzi, and refers to chemical reactions that do not affect the biochemical processes of living systems.¹ This represents a great challenge, as biological systems are extremely complex: they are composed of myriads of small biomolecules with nucleophilic, electrophilic, and redox properties, as well as inorganic ions at different concentrations, and catalytically-active macromolecules –enzymes and enzymatic complexes, many of them with metal-based cofactors–. Biological milieus have also very specific pH and temperature conditions, and they are heavily compartmentalized.

The first bioorthogonal reactions were initially developed as probing methods for monitoring biological processes,² but other applications have emerged since then, such as intracellular drug activation for targeted therapy, and *in situ* generation of imaging probes for diagnosis.³ The introduction of the concept of bioorthogonality opened the door to a new field fresh for improvement, and its importance was most recently highlighted with the awarding of the 2022 Nobel Prize in Chemistry to Bertozzi –shared with Sharpless and Meldal–, with emphasis on the conceptual nature of her contributions.⁴

Bioorthogonal reactions are usually required to possess the following characteristics:^{5–7}

- Chemoselectivity: the reactants do not present side reactions with components of the biological system –that means they are biologically inert– and react only with their corresponding reaction partners.
- Biocompatibility: the reaction must take place at biological conditions of aqueous medium, pH and temperature. Also, the reactants and reagents should be non-toxic at the required concentrations and stable in biological media.
- Fast kinetics: a high reaction rate helps avoiding undesirable side reactions, and it is also necessary for the reaction to successfully take place when the reactants are present at very low concentrations (typical conditions to prevent toxicity).

The first bioorthogonal reaction to be reported was the Staudinger ligation between an azide and a triphenylphosphine.⁸ Subsequently, metal catalysts have been successfully employed both for bioorthogonal reactions that involve either bond formation (copper-catalyzed azide-alkyne cycloaddition (CuAAC),⁹ palladium-catalyzed cross-coupling reactions,^{10,11} ruthenium-catalyzed cross-metathesis reactions)¹² or

cleavage reactions (ruthenium-^{13,14} or palladium-catalyzed deallylation,¹⁵ palladium-catalyzed depropargylation).¹⁶ Other metal-free bioorthogonal reactions have also been developed, like strain-promoted cycloadditions between strained cycloalkynes and 1,3-dipoles (SPAAC),¹⁷ and the inverse electron-demand Diels-Alder (IED-DA) reaction.¹⁸

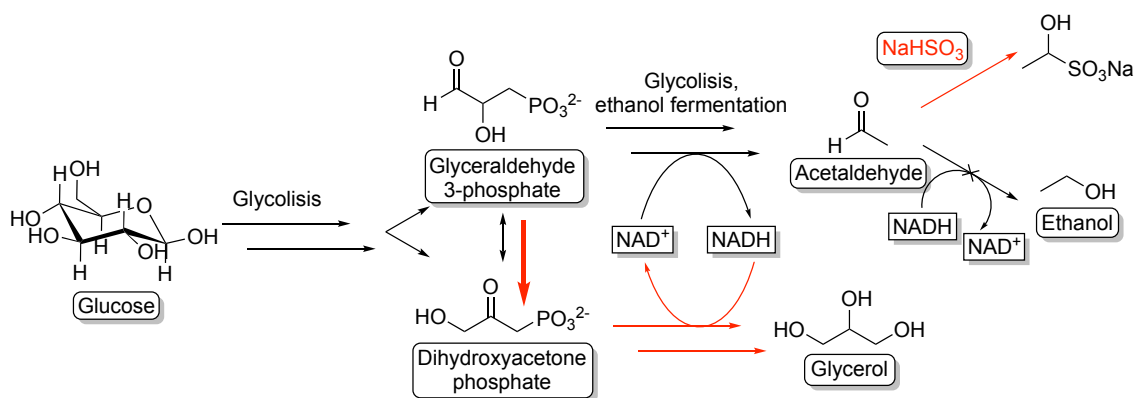
1.2. Biocompatible chemistry

1.2.1. Definition and applications of biocompatible chemistry

Biocompatible chemistry refers to non-enzymatic chemical reactions that can occur under mild conditions and are compatible with living systems.¹⁹ Depending on the authors, the same reactions and experimental settings have been described either as *bioorthogonal* or *biocompatible*, but biocompatible reactions do not necessarily fit all the requirements of bioorthogonal chemistry.

Abiotic biocompatible reactions that interface with the metabolism would offer new possibilities for interrogating or manipulating biological systems and contributing to synthetic biology. These reactions could have biomedical applications, such as in new therapies and diagnostic imaging, and provide valuable tools for basic research in biology. Abiotic biocompatible chemistry also offers the possibility of interfacing synthetic chemistry and synthetic biology, potentially increasing the number of reactions obtainable through biological systems with the far more ample repertoire of classical organic synthesis.^{20,21}

A first report on the biocompatible manipulation of cellular metabolism by non-enzymatic chemistry was reported by Neuberg and Hirsch in 1919. They significantly increased the production of glycerol from glucose by fermentation in *Saccharomyces cerevisiae* in presence of sodium bisulfite (glycerol is a precursor of nitroglycerine, and Neuberg discoveries allegedly benefited the German war effort during the First World War). Bisulfite anion acts as a protecting group for acetaldehyde, blocking the last step of ethanol fermentation and preventing the reoxidation of NADH formed in glycolysis. This promotes the biosynthesis of glycerol via a branching pathway of glycolysis, with concurrent oxidation of NADH to NAD⁺ (Scheme 1).¹⁹



Scheme 1. Neuberg and Hirsch's bisulfite-promoted glycerol production in *S. cerevisiae*. In red, the alternative pathways promoted by addition of bisulfite.¹⁹

Biocompatible abiotic reactions can be promoted by intrinsic redox processes of living systems, or by abiotic catalysts.

1.2.2. Reactions promoted by cellular redox processes

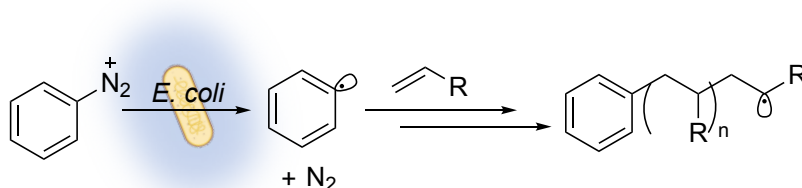
Promoting abiotic reactions by cell-mediated electron transfer has been described as “[o]ne of the simplest and most powerful applications of biocompatible chemistry”.²⁰ Living cells have several ways of donating electrons to promote chemical reactions: they contain oxidizing species, like ROS, as well as a range of reducing biomolecules, such as NAD(P)H and glutathione (GSH), which together contribute to the reducing bulk cytoplasmatic redox potential (the redox state changes inside different organelles, and it also varies between different stages of the cell cycle, cellular lineages and tissue physiological state).²² Eucaryotic cells also possess electron transport chains associated with membranes (in mitochondria and chloroplasts). Additionally, some bacteria possess extracellular electron transfer mechanisms (EET) that enable them to perform anaerobic respiration –that is, to donate electrons at the end of the respiratory chain to an extracellular oxidant different to oxygen, e.g., metal cations like iron(III).²³

Electron transfer from living cells has been until now mainly applied to promote radical polymerization, which is generally compatible with an aqueous milieu. These reactions present limitations, such as the difficulty of monomers to cross the cell membrane (required for intracellular polymerization), quenching of the reaction by oxygen or biomolecules, and the use of UV irradiation²⁴ or toxic metal catalysts.²⁵

The pioneering work of Magennis *et al.*²⁶ employed *Escherichia coli* and *Pseudomonas aeruginosa* to initiate copper-mediated atom transfer radical polymerization (ATRP) of acryloyl monomers. The reductive environment generated by the bacteria continuously reduced Cu(II) to Cu(I), which in turn was oxidated by

abstraction of an halogen atom from an inactive chain end, thus generating a propagating radical chain.²⁶ Subsequent studies with *Shewanella oneidensis* demonstrated that this bacteria's EET machinery –specifically, the outer-membrane cytochrome– was crucial for the promotion of ATRP. The aerobic metabolism of the bacteria was also showed to deplete oxygen, which otherwise would quench the radical polymerization.²⁷

Subsequently, Nothling *et al.*²⁸ were able to perform bacteria-mediated radical polymerization in the absence of metal catalyst, using *Salmonella enterica* serovar Typhimurium and *E. coli*. They employed an arenediazonium salt as an oxidizing agent to hijack the bacterial redox potential and generate the initiating radicals (Scheme 2). The diazonium salt was shown to be biocompatible at concentrations lower than 800 μM . In this case, a reversible addition-fragmentation chain transfer (RAFT) mechanism was selected for the polymerization, which the researchers termed as “BacRAFT”. Mechanistical studies showed that several biological processes could be held accountable for the reduction of the diazonium salt, such as GSH and a key copper oxidase. Nevertheless, a specific mechanism responsible for reducing the diazonium salt was not identified.²⁸



Scheme 2. Bacteria-promoted RAFT polymerization (chain transfer agent not shown).²⁸

ATRP has been also accomplished intracellularly in mammalian cells. Shen *et al.*²⁵ were able to perform polymerization of *N*-hydroxyethylacrylamide with a Cu(II)-histidine complex, from which Cu(I) was continuously generated by endogenous GSH. The *in situ* generation of Cu(I) in catalytic concentrations circumvented its toxicity, and, most important, the reaction was selective to cancer cells, as the tumor microenvironment is reported to include GSH overexpression.^{29,30} The polymerization was further promoted by addition of exogenous sodium ascorbate (NaAsc). The researchers were also able to intracellularly synthesize a new polymer which included Paclitaxel –a chemotherapy agent– and showed a higher apoptosis-inducing effect when compared to that of the monomer. This was attributed to the intracellular retention of the polymerized drug.²⁵

Alternatively, the reducing milieu of the cell can be used for uncaging reactions. This was achieved by Liang *et al.*,³¹ who modified the bioorthogonal condensation of 2-cyano-benzothiazole and the aminothioli moiety of cysteine by protecting the thiol with a disulfide-bonded group which prevented condensation. In the intracellular reducing milieu, the disulfide bond suffered a reductive cleavage which allowed the bioorthogonal reaction to progress.³¹ This method was subsequently employed to selectively induce intracellular polymerization under reducing conditions for photoacoustic imaging.³²

Oxidizing agents can also promote abiotic reactions in biological media. Wang *et al.*³³ achieved intracellular synthesis of a cyanine dye from 1-butyl-2,3,3-trimethyl-3H-indole selectively in mitochondria. The transformation takes place via several radical-radical couplings, and formation of the radical intermediates is promoted by endogenous ROS generated in the mitochondria. The reaction occurs preferentially in cancer cells (HeLa and A549), as they have higher levels of ROS.³³

Oxidizing agents have been employed to promote biocompatible polymerization as well. For example, Zhao *et al.*³⁴ synthesized a phenylboronic acid-protected dopamine which selectively imitated natural synthesis of melanin in high ROS environments. The deprotection of the monomer was induced by ROS, and the subsequent polymerization and final melanin-like structure both presented ROS-scavenging abilities. This modified dopamine was used to successfully treat drug-induced acute liver injury in mice and allowed imaging of the injured liver tissue via near-IR absorbance.³⁴

1.2.3. Reactions promoted by abiotic catalysts

Another approach to performing abiotic biocompatible chemistry consists of the use of artificial non-enzymatic catalysis. For instance, Liu *et al.*³⁵ used Fe(III) as a non-enzymatic biocompatible catalyst for the oxidative decarboxylation of α -acetolactate (produced from glucose by a native metabolic pathway) to give diacetyl in a strain of *Lactococcus lactis* with knockout mutations for competing metabolic pathways. The resulting diacetyl could then be reduced to (*S,S*)-2,3-butanediol by heterologous reductases which conformed another metabolic pathway, so the exogenous catalysis effectively bridged both routes. The second, heterologous route regenerated NAD⁺, thus reestablishing the redox balance in the knockout bacteria.

1.2.4. Future projection of abiotic biocompatible chemistry

Biocompatible abiotic chemistry has experienced great progress in the last years, but many of its possibilities remain undoubtedly unexplored and unexploited. There has

been little research on biocompatible, living-system-promoted synthesis of small molecules –particularly via bond forming reactions–, and on biocompatible reactions in mammalian cells, even though those fields are recognized as very promising.^{19–21} Until now, research has been conducted mainly in bacteria, as they are generally more tolerant to exogenous chemicals and require less restrictive culture conditions than eucaryotic cells. On the other hand, biocompatible reactions in mammalian cells would potentially provide more relevant biomedical applications.

Besides, the quantitative extent of biocompatible processes has rarely been reported. This is crucial to properly evaluate and compare each method. Several techniques have been proposed for quantifying the yield of biocompatible reactions, such as mass spectrometry, liquid chromatography, and radiometric imaging.²¹

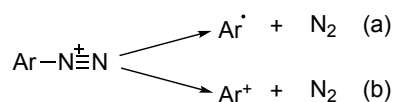
1.3. Chemistry of arenediazonium salts

1.3.1. General reactivity of arenediazonium salts

Diazonium salts are widely used in organic synthesis, as they present several advantages: they are easily obtained, react at room temperature, and their reactions usually proceed with the extrusion of N₂ –a very inert gas– and are generally very chemoselective.³⁶ Arylation reactions by arenediazonium compounds have great interest because of the wide presence of aryl groups in drugs and natural products.³⁷

Reactions of arenediazonium salts can be classified in nitrogen-retention and dediazonation reactions.³⁸ In nitrogen-retention reactions, arenediazonium salts act as electrophiles. A classic example is the diazo coupling with activated arenes, which is widely used to synthesize dyes.³⁹

Reactivity of arenediazonium compounds can also proceed by dediazonation (extrusion of N₂). The dediazonation may take place either by homolytic or heterolytic cleavage to give, respectively, an aryl radical or an aryl cation (Scheme 3). Homolytic cleavage is a redox process, so it requires an electron transfer.⁴⁰



Scheme 3. Homolytic (a) and heterolytic (b) dediazonation.⁴⁰

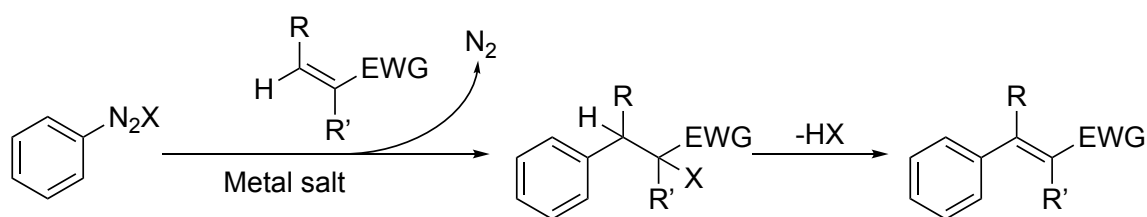
Homolytic dediazonation can be induced by metal cations⁴⁰ (e.g. in the Sandmeyer reactions to give chloro- and bromobenzenes, in the classical Meerwein arylation, and also in several palladium-catalyzed cross-coupling reactions).³⁷ It can also be achieved

by thermal or photochemical decomposition (arenediazonium salts usually absorb UV light).³⁶ In both cases, the mechanism depends heavily on the solvent and the anion.⁴¹

In recent years, photocatalysis has been used increasingly to generate aryl radicals from diazonium salts in a controlled way, at low temperature, and employing visible light as an affordable source of energy. The use of both metal complexes (e.g. Ru(bpy)₃) and organic dyes (e.g. eosin Y) has been reported.^{37,42}

1.3.2. The Meerwein arylation

The Meerwein arylation was originally reported in 1939 as the arylation of an electron-poor alkene catalyzed by Cu(II) salts (Scheme 4). The original reaction had some drawbacks, such as its limited substrate scope, low yields, and side reactions, although several advances have been achieved with different reducing agents and improved conditions.^{36,43} Photocatalytic Meerwein arylations have been reported, both with Ru(bpy)₃ and eosin Y photocatalysts.⁴³



Scheme 4. Schematic representation of a Meerwein arylation.

2. Objectives and work plan

2.1. Objectives

This Degree Final Project aims to present new carbon-carbon bond forming biocompatible synthetic reactions within mammalian cells by harnessing the redox cell machinery. Specifically, we aim: (1) to promote the Meerwein arylation of 2-(4-methoxyphenyl)naphthalene-1,4-dione with *p*-methoxyaryldiazonium tetrafluoroborate by the cell machinery in eukaryotic cells (HeLa, A549) and prokaryotic organisms (*E. coli*); (2) to shed light into the mechanism of the reaction in cell environments; (3) to study the mechanism of the reaction outside cells in abiotic media (from now on, referred as *in vitro*) in the presence of biological reducing agents; (4) to expand the scope of intracellular biocompatible reactions based on diazonium salts.

2.2. Work plan

Table 1. Work plan.

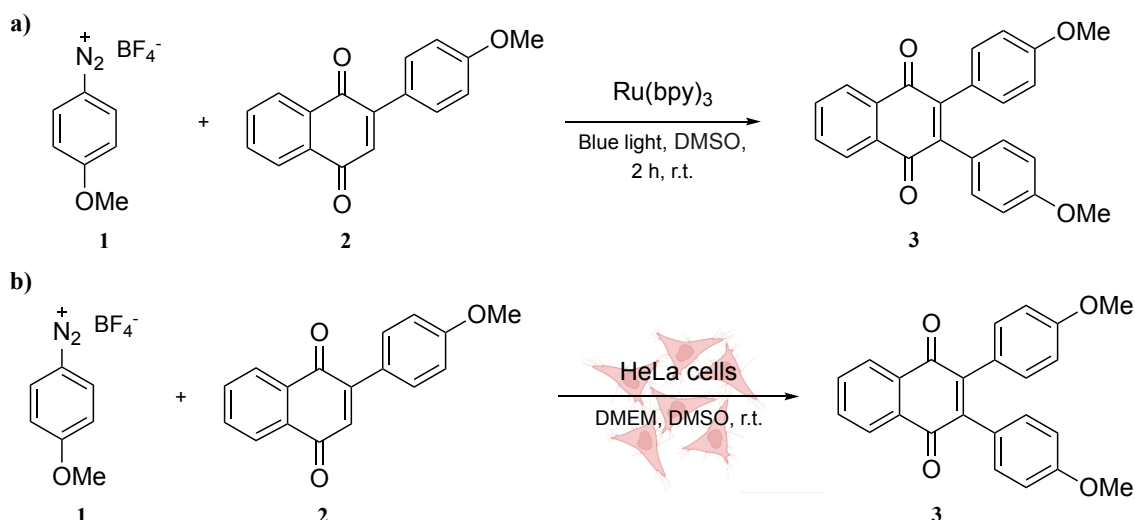
Month	Task
November	– Bibliographical research (Chemistry) – Familiarization with the lab
December	– Synthesis of reactants 1 and 2
January	– Bibliographical research (Biology)
February	– Evaluation of the photocatalytic reaction
March	– Screening of biological reductants
April	– Optimization of conditions for best reductant
May	– Mechanistic studies <i>in vitro</i> – Evaluation of alternative acceptors and reactions
June	– Experiments in eukaryotic and procaryotic cells

3. Results

3.1. (Non-)Photocatalyzed reactions in cells: a frustrating finding.

With the aim of developing new biorthogonal transformations, the group of Prof. J. L. Mascareñas decided to explore visible-light-mediated, photoredox catalytic reactions like the photocatalyzed Meerwein arylation shown in Scheme 5a, which involves the use of a ruthenium complex and aryl diazonium salts as radical sources. In this search, they observed an interesting but totally unexpected result: the reaction took place directly in live cells, providing the final naphthoquinone **3** without the need of neither light nor the Ru complex (Scheme 5b). Surprisingly, the cell was able to promote the transformation. This exciting finding represents the first synthetic carbon-carbon bond-forming reaction prompted by the cell machinery, and therefore the group initiated a research program in the topic. Very likely, the reaction is driven by the redox potential of the cell.

The work was carried out in collaboration with PhD student Fernando Salgado.



Scheme 5. (a) Initial attempts to develop bioorthogonal photocatalysis in live cells. (b) This work: developing new biocompatible transformations promoted by the live cell machinery.

3.2. Evaluation of the photocatalyzed reaction

The initial efforts were focused on investigating this Meerwein arylation between *p*-methoxyaryldiazonium tetrafluoroborate (**1**) and 2-(4-methoxyphenyl)naphthalene-1,4-dione (**2**) (Scheme 5a).

First attempts were carried out by dissolving compounds **1** (1 eq., 10 mM), **2** (3 eq.) and Ru(bpy)₃ (0.05 eq.) in deoxygenated DMSO (1 mL) under inert atmosphere and irradiating with blue light (450 nm, 60 mW/cm²). All components were apparently soluble in the choice solvent. A ratio 3:1 of naphthoquinone / diazonium salt had been previously demonstrated to be necessary to achieve high yields. Adequate controls were performed in the absence of photocatalyst and illumination. Yield of **3** was determined by ¹H-NMR with dibromomethane as internal standard, unless otherwise noted. Results are summarized in Table 2.

The arylated naphthoquinone **3** was obtained in 85% yield after 2 h under irradiation in presence of Ru(bpy)₃ (entry 1). Bubbling due to the extrusion of nitrogen was immediately observed, and the solution turned from orange to dark red in 10 min. In the absence of blue irradiation, trace amounts of the product were observed, either under the lab's ambient illumination (entries 2 and 5) or in total darkness (entries 3 and 6). Surprisingly, a yield of 63% (isolated yield of 38%) was obtained under blue illumination in the absence of catalyst (entry 4).

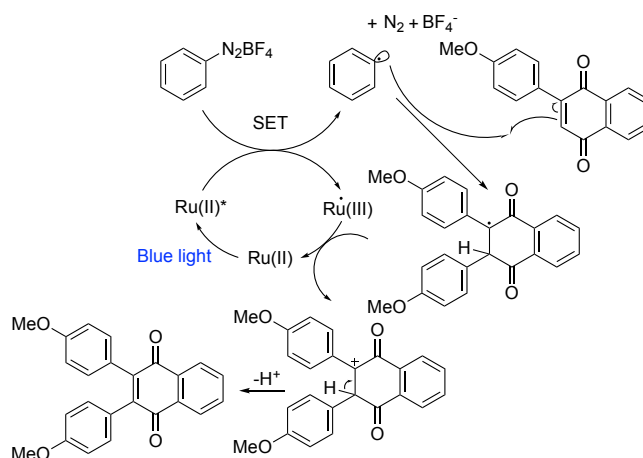
Table 2. Evaluation of the photocatalyzed reaction.^a

Entry	Catalyst	Illumination	Time/h	Yield of 3/%
1	Ru(bpy) ₃	Blue	2	85
2	Ru(bpy) ₃	Ambient	2	Traces
3	Ru(bpy) ₃	Darkness	2	Traces
4	-	Blue	2	63 (38 isolated)
5	-	Ambient	2	Traces
6	-	Darkness	2	Traces

(a) Reaction conditions (unless otherwise noted): **1** (1 eq., 10 mM), **2** (3 eq.), Ru(bpy)₃ (0.05 eq.), DMSO (entries 1–3 and 5–6: 1 mL; entry 4: 20 mL), r.t., inert atmosphere. Yields determined (unless otherwise noted) by ¹H-NMR using dibromomethane as internal standard. Traces defined as less than 7% yield.

In 2022, Nagar and Dhar⁴⁴ reported the photocatalyzed arylation of naphthoquinones using eosin Y (EY) as photocatalyst under green irradiation. Surprisingly, they did not observe any conversion in the absence of catalyst.

These authors proposed a mechanism for their reaction under EY catalysis and green light, and an adapted mechanism is here proposed for the Ru(bpy)₃-catalyzed reaction (Scheme 6). After excitation of the photocatalyst, the reaction would begin with a single electron transfer (SET) from the excited Ru(II) complex to **1**, which generates an aryl radical by nitrogen extrusion, and Ru(III). The aryl radical is trapped by **2** to give a new radical species. The catalytic cycle closes with a new SET from this species to Ru(III) to regenerate Ru(II) and give a carbocation, which deprotonates to yield product **3**.⁴⁴



Scheme 6. Proposed mechanism for the photocatalyzed Meerwein arylation using Ru(bpy)₃ as catalyst, based on the mechanism proposed for the eosin Y-catalyzed reaction.⁴⁴

Assuming that the blue light-promoted reaction also proceeds via an aryl radical in the absence of catalyst, it seems unlikely that either the BF_4^- counterion or the solvent participate directly in the electron transfer process. In 2021, Witzel *et al.*⁴⁵ had reported the arylation of furan by tetrafluoroborate arenediazonium salts in methanol under blue illumination. The transformation did not take place in DMSO. That was explained by the absence of light absorption of arenediazonium salts and DMSO in that range of the spectrum, while methanol can absorb blue light.

In the case of arylation of naphthoquinone derivatives, the aryl radical may be generated by interaction with the naphthoquinone **2**, which would act as the photocatalyst. Wang *et al.*⁴⁶ reported a similar case in which boron dipyrromethene dyes self-promoted their arylation with diazonium salts when excited with visible light. Nevertheless, more research is needed to clarify this point, but, although the possibility of a new catalyst-free photoinduced arylation of naphthoquinones is interesting, it falls out of the scope of the present work.

3.3. *In vitro* experiments

3.3.1. *Screening of different biological reductants*

Living cells contain several reducing biomolecules of low molecular weight that serve as coenzymes in multitude of redox enzymatic reactions (both prosthetic groups permanently bounded to proteins, and free coenzymes which are transitorily attached to enzymes), and also as antioxidants that remove harmful ROS from the cell. Aryldiazonium salts are known oxidants, and it has been reported that some biological reductants are able to reduce aryldiazonium compounds to aryl radicals.⁴⁷ It was thus hypothesized that low-weight reducing biomolecules could be directly responsible for promoting this Meerwein arylation between **1** and **2**.

Three biomolecules were selected to test their ability to promote the reaction in abiotic conditions: glutathione (GSH), nicotinamide-adenine dinucleotide (NADH) and ascorbate.

GSH is the main antioxidant present in cells.⁴⁸ It is a tripeptide with structure γ -L-glutamyl-L-cysteinyl-glycine (Figure 1a). Its oxidation proceeds by disulfide bond formation between the thiol groups of two molecules of GSH to give glutathione disulfide. The usual concentration of GSH in the cytoplasm ranges between 0.1–10 mM,⁴⁹ although in most cells the concentration is 1–2 mM.⁴⁸ However, GSH has been found in elevated concentrations in several types of cancer.²⁹ GSH concentration

and GSSG/GSH ratio are considered important indicators of the cytosolic redox state,⁴⁹ and concentrations of GSSG are usually very low, of 5–10% of the total.⁴⁸

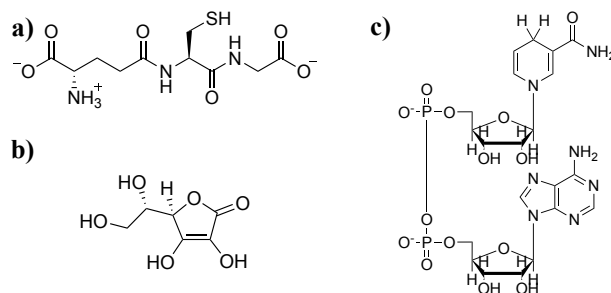


Figure 1. Structures of biological reductants: (a) L-glutathione; (b) NADH; (c) ascorbate.

NADH (Figure 1b) is the main redox coenzyme of the cell. It is formed by two 5'-phosphate nucleosides: adenosine 5'-phosphate and another 5'-phosphate nucleoside containing nicotinamide at the 1' carbon. The nucleosides are joined by an ester bond between the phosphates. NADH is oxidized by net donation of a hydride (H^-) to give NAD^+ . Cellular concentration of NAD^+ averages $365 \mu\text{M}$,^{50,51} with a NAD^+/NADH ratio of around 10:1,⁵² but these values vary greatly between organelles: for the cytoplasm, the values of $50 \mu\text{M}$ ⁵³ and a 600–700:1 ratio^{54,55} have been reported for free (non protein-bounded) NAD^+ and NADH, and the corresponding values for mitochondria are $246 \mu\text{M}$ ⁵⁶ and 8:1.⁵⁴ Moreover, NADH has been reported to generate aryl radicals from aryl diazonium salts in abiotic conditions.⁴⁷

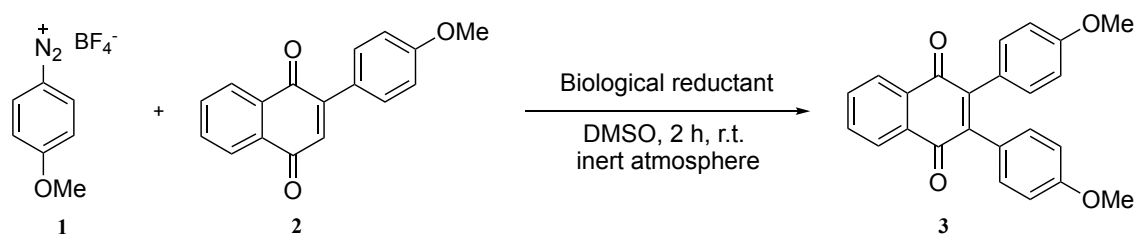
Ascorbate (Figure 1c), also known as vitamin C, serves as a coenzyme and an antioxidant. Its concentration in mammalian cells is in general 1–5 μM , although specific cell types can reach 10 mM or more.⁵⁷ Ascorbate has also been reported to generate aryl radicals by reduction of arenediazonium compounds in abiotic media.⁴⁷

The ability of these three selected biological reductants to promote this Meerwein reaction was then explored. NADH disodium salt and sodium ascorbate (NaAsc) were used as sources for NADH and ascorbate, respectively. Compounds **1** (1 eq., 10 mM), **2** (3 eq.) and the biological reductant (1 eq.) were dissolved in 1 mL of DMSO or DMSO:H₂O (1:1) under inert atmosphere (Table 3). All reductants were apparently soluble in DMSO. However, naphthoquinone **2** was insoluble in this mixture of DMSO:H₂O. Yield of **3** was determined by ¹H-NMR with dibromomethane as internal standard.

All three reductants were found to promote the reaction, both in absence and presence of water. The decreased yields in the latter case were attributed to the poor solubility of compound **2** in water. The highest yields were obtained for NADH in both

conditions (77% in DMSO, entry 3, and 36% in DMSO:H₂O, entry 4). For this reason, NADH was selected for the study of the *in vitro* reaction, and new experiments were conducted to optimize conditions for the NADH-promoted reaction.

Table 3. Screening of biological reductants.^a

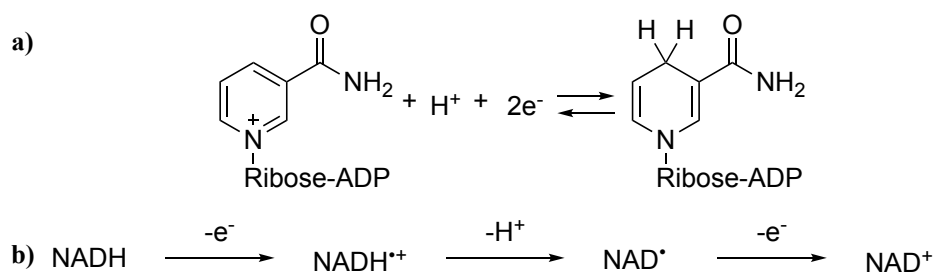


Entry	Additive	Water/%	Yield/%
1	GSH	0	53
2	GSH	50	12
3	NADH	0	77
4	NADH	50	36
5	NaAsc	0	33
6	NaAsc	50	28

(a) Reaction conditions (unless otherwise noted): **1** (1 eq., 10 mM), **2** (3 eq.), additive (1 eq.), DMSO or DMSO:H₂O (1 mL), 2 h, r.t., inert atmosphere, ambient light. Yields determined by ¹H-NMR using dibromomethane as internal standard.

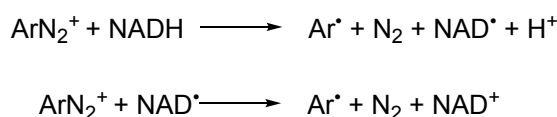
3.3.2. Optimization of conditions and study of the NADH-promoted reaction

The reversible oxidation of NADH (Scheme 7a) takes place with the transference of two electrons and a proton, but it is still debated whether the electron transference is concerted or stepwise (Scheme 7b).⁵⁸ These two mechanisms can be also thought of as extremes of a continuous spectrum,⁵⁹ and the observation of one or the other would depend in each case of the rate constants for each elementary step.⁶⁰ Nonetheless, the radical NAD[•] has been identified in enzymatic⁶⁰ and non-enzymatic reactions.⁶¹



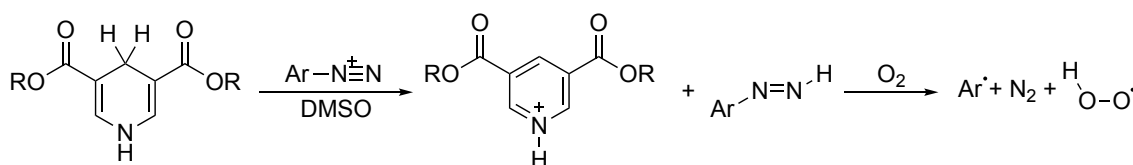
Scheme 7. (a) Redox NAD⁺/NADH pair.⁶² (b) Stepwise mechanism for NADH reduction.⁶⁰

Regarding the reduction of arenediazonium compounds, Yasui *et al.*⁵⁹ suggested an outer sphere SET mechanism for dediazonation promoted by BNAH (a NADH analogue). Substoichiometric amounts of BNAH would initiate a free radical chain which is inhibited by oxygen, and also by stoichiometric or higher than stoichiometric quantities of BNAH. Reszka and Chignell⁴⁷ hypothesized that generated NAD[•] would in turn react with another diazonium cation, as it is a powerful oxidizing agent (Scheme 8).



Scheme 8. NADH-promoted homolytic dediazonation by outer sphere SET.⁴⁷

On the other hand, Tatunashvil *et al.*⁶³ have reported that Hantzsch ester, which is a stronger hydride donor than NADH,⁶⁴ induces fragmentation of arenediazonium compounds to give aryl radicals via a hydride transfer mechanism. They observed that the reaction only took place in presence of oxygen, and proposed a mechanism in which oxygen induced the fragmentation of an arenediimide intermediate (Scheme 9).



Scheme 9. Formation of aryl radicals from arenediazonium cations by hydride transfer from Hantzsch ester followed by oxygen-mediated fragmentation of intermediate diimide.⁶³

To get more information about the reaction, different experiments were performed changing the concentration of NADH. Besides, to study the role of oxygen in the process, the influence of using deoxygenated solvents as well as nitrogen or open-air atmosphere was explored (Table 4). The yield of **3** increased using higher quantities of NADH (entries 1–6) until reaching a maximum at 1.0 eq. (entries 5–6). Lower yields of product **3** were formed with superstoichiometric amounts of the reducing agent (entries 8–9). This could be explained by a «discoordination» between the aryl radical generation and the radical attack to the double bond of **2**. In the presence of more than equimolar quantities of NADH, the aryl radical will probably form faster, which can in turn favor competitive reactions.

Deoxygenation of the solvents gave higher yields when substoichiometric quantities of NADH were used (entries 1–4), but almost no difference was observed for 1.0 eq. of NADH (entries 5–6). When the reaction was carried out under open

atmosphere, a slightly reduced yield was observed (entry 7). These findings support the outer sphere SET mechanism, as oxygen is not necessary for the reaction to proceed. Inhibition by oxygen is probably due to trapping of intermediate radicals. Addition of TEMPO, a radical trapping agent, also lowered the yield (entries 10–12), which corroborates the participation of radicals in the process.

Table 4. Optimization of reaction conditions with NADH.^a

Entry	NADH/eq.	Deoxygenation	Atmosphere	Yield/%
1	0.1	Yes	N ₂	56
2	0.1	No	N ₂	43
3	0.8	Yes	N ₂	58
4	0.8	No	N ₂	67
5	1.0	Yes	N ₂	72
6	1.0	No	N ₂	77
7	1.0	No	Open	65
8	1.5	Yes	N ₂	65
9	2.0	Yes	N ₂	39
10	0.1	Yes	N ₂	19 ^b
11	1.0	No	N ₂	58 ^b
12	1.0	No	N ₂	27 ^c

(a) Reaction conditions (unless otherwise noted): **1** (1 eq., 10 mM), **2** (3 eq.), DMSO (1 mL), 2 h, r.t., inert atmosphere, ambient light. (b) 1 eq. of TEMPO. (c) 10 eq. of TEMPO. Yields determined by ¹H-NMR using dibromomethane as internal standard.

The reaction time was next investigated. A substantial yield of 56% was achieved with substoichiometric amounts of NADH after 2 h (0.1 eq, Table 4, entry 1), and similar results were obtained with reduced reaction times of 1 h or 30 min (Table 5, entries 1–2). Indeed, the HPLC-MS analysis of reaction crude for a 1 h reaction with 1.0 eq. of NADH showed that NADH was completely consumed, as only NAD⁺ (m/z of 664) was detected (Table 6). This suggests that, in abiotic conditions, NADH acts as radical initiator for a radical chain process.

Table 5. Yields at different times with NADH.^a

Entry	NADH/eq.	Time/min	Yield/%
1	0.1	30	54 ^b
2	0.1	60	53 ^b
3	1.0	1	29
4	1.0	5	64
5	1.0	10	67

(a) Reaction conditions (unless otherwise noted): **1** (1 eq., 10 mM), **2** (3 eq.), NADH, DMSO (1 mL), r.t., inert atmosphere, ambient light. (b) Deoxygenated solvent. Yields determined by ¹H-NMR using dibromomethane as internal standard.

To further test this hypothesis, an experiment was devised in which a second equivalent of diazonium salt **1** was added after 1 h to the reaction with 0.1 eq. of NADH. An increment in the yield from 0.56 eq. to 0.76 eq. was observed, proving that radical intermediates remained in the reaction milieu and were able to promote the fragmentation of the additional quantity of **1**.

The reaction was also evaluated for 1.0 eq. of NADH at different reaction times, showing the fast kinetics of the process. After 10 minutes, there were almost no changes in the yield obtained (Table 5, entries 3–5).

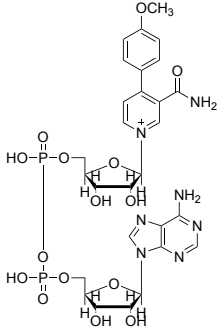
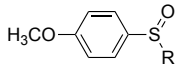
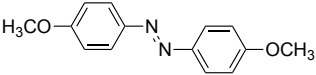
The reaction was also attempted with naphthoquinone **2** as limiting reactant (10 mM of **2**, 3.0 eq. of **1**, 0.1 eq. of NADH, deoxygenated solvent), obtaining a decreased yield of 32%. This is explained because aryl radicals are highly reactive species, and an excess of the acceptor alkene **2** is necessary for the reaction to adequately compete with side reactions.

Additional experiments were conducted to determine the water sensitivity of the reaction. As previously mentioned, 50% of water decreased the reaction yield from 77% to 36% (Table 3, entries 3–4). However, the same yield of 36% was obtained when water content was reduced to 10% in the same conditions. The reaction was also attempted in other organic solvents (acetonitrile and THF), but only trace amounts of product were observed. This was attributed to the poor solubility of NADH in both solvents.

Therefore, after the exhaustive optimization process, the optimized conditions were selected as 10 mM of **1**, 3 eq. of **2**, 1 eq. of NADH, DMSO, 2 h, r.t. and inert atmosphere.

To further evaluate the mechanism, identification of reaction subproducts was attempted. In order to monitor the process by $^1\text{H-NMR}$, the optimized reaction was carried out in $\text{d}_6\text{-DMSO}$, but a very complex spectra was obtained, and no new species could be positively identified.

Table 6. Identification of subproducts by HPLC-MS

Species	Detected masses/m/z	Conditions
NADH	666 (M+1)	a,b
NAD ⁺	664 (M+1), 123 (nicotinamide+1)	c–f
	770 (M+1), 542 (M–nicotinamide–PhOCH ₃), 229 (nicotinamide+PhOCH ₃ +1), 108 (PhOCH ₃ +1)	d,f
	R = CH ₃ 171 (M+1), 154 (M–CH ₃) R = CD ₃ 174 (M+1), 157 (M–CD ₃)	c,e d,f
	243 (M+1)	c–f

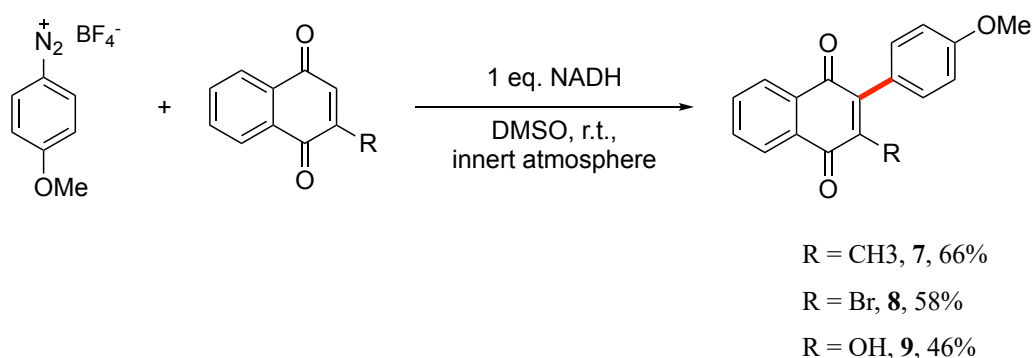
Conditions: 1 mL, 1 h, r.t., inert atmosphere, ambient light. (a) NADH (10 mM), DMSO. (b) NADH (10 mM), $\text{d}_6\text{-DMSO}$. (c) **1** and NADH (both 10 mM), DMSO. (d) **1** and NADH (both 10 mM), $\text{d}_6\text{-DMSO}$. (e) **1** (10 mM), **2** (30 mM) and NADH (10 mM), DMSO. (f) **1** (10 mM), **2** (30 mM) and NADH (10 mM), $\text{d}_6\text{-DMSO}$.

In contrast, HPLC-MS allowed for identification of several subproducts (Table 6). The detection of aryl methyl sulfoxide (**5**) in all reactions is consistent with reports of $\text{Ru}(\text{bpy})_3$ -and-light-catalyzed methylsulfoxidation of arenediazonium salts.⁶⁵ Methylsulfoxidation could thus represent an important side reaction in the selected conditions. Additionally, in those transformations carried out in deuterated solvent, a compound with mass that could agree with that of the product of arylation of NAD⁺ in position 4 of the nicotinamide (**4**) could be detected. A possible mechanism for this

transformation would be the radical coupling of NAD^\bullet and the aryl radical derived from the diazonium salt. This would contribute to explaining the decrease in yield when more than 1 eq. of NADH is used, since NADH would be capturing the aryl radicals.

3.3.3. Evaluation of alternative acceptors

Three 1,4-naphthoquinones which were available at the lab were evaluated *in vitro* to widen the scope of the transformation (Scheme 10). Products were not isolated, as this was a first preliminary test, and the yield was determined by $^1\text{H-NMR}$ comparing with the reported spectra. Reactions with naphthoquinones proceeded with acceptable yields, but lower than for derivative **2**.



*Scheme 10. NADH mediated arylation reactions of three different 1,4-naphthoquinones. Reaction conditions: **1** (1 eq., 10 mM), starting naphthoquinone (3 eq.), NADH (1 eq.), DMSO (1 mL), r.t., inert atmosphere, ambient light. Reaction time was 4 h for **7** and 2 h for **8** and **9**. Yields determined by $^1\text{H-NMR}$ using dibromomethane as internal standard. Peaks were identified by comparison with reported spectra.*

3.3.4. Reactions with alkynes

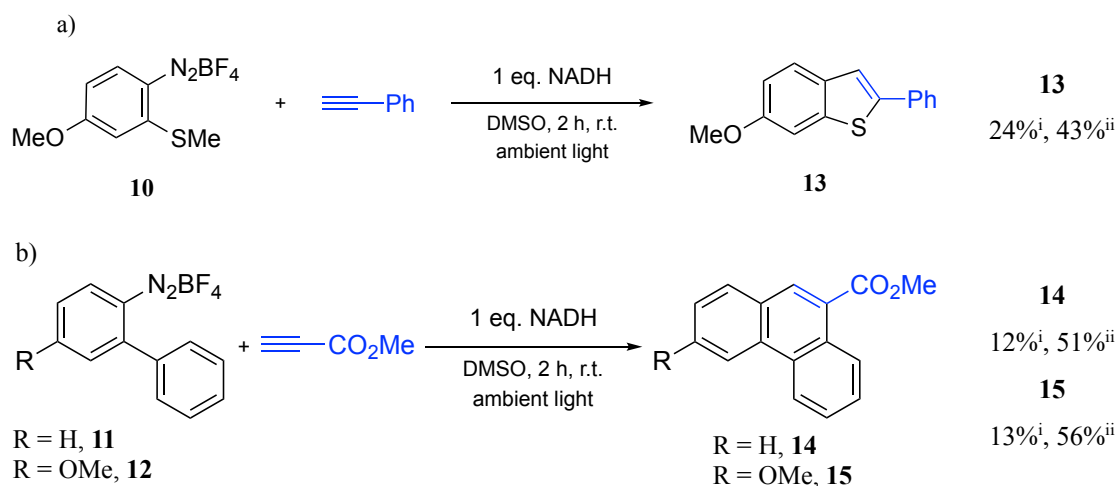
Several photocatalytic reactions between arenediazonium salts and alkynes have been reported. Some of these transformations have been previously studied in the research group as candidate bioorthogonal reactions, so three adequate aryldiazonium salts (**10–12**) were already synthesized and were generously shared.

Hari *et al.*⁶⁶ demonstrated that benzothiophenes can be synthesized from alkynes and 1,2-methylthioarenediazonium salts employing green light and EY as photocatalyst. The reaction was thus attempted using diazonium salt **10** and phenylacetylene in presence of NADH. An initial yield of 24% was determined for **13**, but an increase from 3 to 10 eq. of the alkyne gave a yield of 43% (Scheme 11a).

Xiao *et al.*⁶⁷ also reported synthesis of phenanthrenes by cascade radical reactions initiated by EY and visible light. In this case, treatment of diazonium salts **11** and **12** and

methyl propiolate employing NADH as initiator afforded low yields, which could be improved when the quantity of alkyne was increased from 3 to 10 eq. (Scheme 11b).

These results suggest that the reactions could also be promoted by cells, potentially widening the scope of biocompatible transformations based on aryldiazonium salts.



Scheme 11. NADH promoted reaction of arenediazonium salts and alkynes. Reaction conditions: 10–12 (1 eq., 10 mM), alkyne ((i) 3 eq. or (ii) 10 eq), NADH (1 eq.), DMSO (1 mL), 2 h, r.t., inert atmosphere, ambient light. Yields determined by ¹H-NMR using dibromomethane as internal standard. Peaks were identified by comparison with reported spectra.

3.4. Experiments in cells

3.4.1. ATP viability assay

The toxicity of reactants and product was evaluated by means of an ATP cell viability assay. ATP is the main cellular energy currency, and, as cells become damaged or die, they lose the ability to synthesize it, so their ATP levels drop. ATP is thus a good indicator of the metabolic capacity of the cell.⁶⁸

HeLa cells were incubated for 1 h in DMEM with 0.5% v/v of DMSO and 100 μM of **1**, **2** or **3**, and also with **1** and **2** simultaneously, to study the effect of the reaction. DMSO, reported to be nontoxic to HeLa cells under 2% v/v concentration,⁶⁹ was employed as cosolvent because of the poor water solubility of compound **2**. A second assay was undertaken in which cells were subjected to starvation for the night before by changing the culture medium for DMEM with 1% FBS (fetal bovine serum). Starvation is usually employed to synchronize cultured cells in the same cell cycle stage,⁷⁰ but it also induces generation of ROS.⁷¹ The results of both assays are shown in Figure 2a.

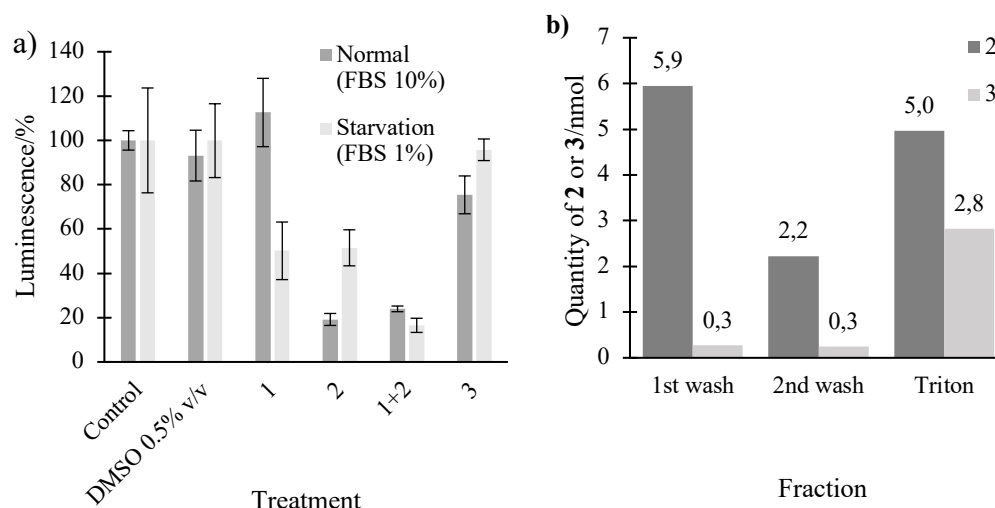


Figure 2. (a) ATP viability luminescence assay in HeLa cells. Values of luminescence are normalized for those of the corresponding controls. FBS: fetal bovine serum. Compounds **1**, **2** and **3** at 100 μM . 0.5% DMSO was used in all treatments except in controls. (b) Quantification of reactant **2** and product **3** in HeLa cells incubated in DMEM with 100 μM of compounds **1** and **2** and 0.5% DMSO for 1 h. 114.5 nmol of **2** and 0.6 nmol of **3** were recovered from the culture medium (values not shown).

The experiment corroborated that DMSO does not affect viability at the concentrations employed. It also confirmed that, in normal conditions, compound **1** does not affect viability, while compound **2** reduces viability in 81%. When incubating cells with compounds **1** and **2** simultaneously, viability also decreases, but less than when incubating cells only with **2**. This could reflect the consumption of toxic compound **2** due to the formation of product **3**, which is less toxic (viability of 80%). Surprisingly, compound **1** does present toxicity when cells are in starvation. It is possible that the diazonium salt **1** is affecting the cells' ability to properly regulate oxidative stress under high stress conditions.

3.4.2. Evaluation of the reaction in HeLa cells

As preliminary studies showed that the Meerwein arylation between compounds **1** and **2** could be promoted by the cell machinery, the reaction was evaluated in HeLa cells.

HeLa cells were incubated for 1 h with 100 μM of the reactants in fresh DMEM with 0.5% v/v of DMSO. After incubation, the culture media was collected. Cells were washed two times with fresh PBS and lysed with Triton X-100 to extract compounds **2** and **3**. The culture media, the two washings and the extraction fraction were analyzed by HPLC-MS, to detect the formation of product **3** as well as the presence of compound **2**. Diazonium salt **1** could not be observed due to its decomposition in the cell environment.

Moreover, compounds **2** and **3** could be quantified using coumarin as internal standard using appropriate calibration curves (Figure 2b. See detailed procedure on subsection 3.5.11).

2.8 nmol of product **3** and 5.0 nmol of reagent **2** were recovered in the extraction with Triton, which is the most representative of the cell contents. In contrast, almost no product **3** was found on the culture medium and the two washings, while high quantities of compound **2** were recovered from them. This opposite distribution of the reactant and the product suggests that the reaction occurs intracellularly. A tentative intracellular yield of 36% can be calculated considering only the values for the extraction with Triton, but these are preliminary results, and the extraction and quantification methods are still not optimized. Undergoing research suggests that acetonitrile would be a much more effective extraction solvent than Triton.

3.4.3. Cell fractionation experiments

The interior of the eucaryote cell is divided by lipidic membranes into specialized compartments with various functions. These subcellular structures maintain differential concentrations of small solutes and incorporate specific proteins.⁷² That represents a main difficulty for translating chemical reactions from reaction flasks to cellular media.

Mitochondria are the organelles that harbor the electron transport chain (ETC), which is responsible for generating the most part of metabolic power in eukaryotic cells, and they are also the main site for cellular ROS production.⁷³ It was thus hypothesized that mitochondria could be responsible for the intracellular promotion of the arylation reaction. To test this hypothesis, a cell fractionation experiment was devised. Cell fractionation techniques allow for the separation of subcellular structures while maintaining their functionality.⁷⁴

A culture of A549 cells was fractionated using a commercial mitochondria isolation kit. The obtained isolated mitochondria and cytosolic fraction were incubated with 100 μM of compounds **1** and **2**. A second mitochondrial fraction was subjected to sonication to break the organelle's membranes. This fraction of lysed mitochondria was also incubated with 100 μM of compounds **1** and **2**. A culture of A549 cells was used as control in the same incubation conditions. All experiments were undertaken in 1.6 mL of PBS with 0.5% v/v of DMSO, with an incubation time of 1 h at 37 °C. After incubation, cultures with whole structures (isolated mitochondria and the control with whole cells) were centrifugated, and the culture media were retired. The remaining pellets, composed

either by mitochondria or cells, were washed with PBS and centrifugated again. The culture media, the washings and the pellets were analyzed separately by HPLC-MS. On the other hand, the cytosolic fraction and the lysed mitochondria, which did not contain whole cells nor intact subcellular structures, were analyzed directly (see detailed procedure on subsection 3.5.12). Qualitative results are summarized in Table 7.

Table 7. Qualitative results for the reaction in isolated mitochondria, lysed mitochondria, and cytosolic fraction of A549 cells. ✓ and X indicate detection or not of compounds 2 or 3.

Fraction	Pellet		Medium		Washing	
	2	3	2	3	2	3
A549 cells	✓	✓	✓	✓	✓	✓
Isolated mitochondria	X	X	✓	✓	✓	✓
Lysed mitochondria	-	-	✓	✓	-	-
Cytosolic fraction	-	-	✓	X	-	-

The reaction took place both in presence of isolated mitochondria and lysed mitochondria (the fact that neither the product 3 nor compound 2 were found in the mitochondria pellet is clearly an error in the determination, as the originally white pellet was colored yellow after treatment, indicating the presence of precipitated 2). Additional experiments are required to determine the role of the ETC, either by removing the membranes from the mitochondria lysate, or by blocking the ETC in isolated mitochondria with inhibitors such as Antimycin A or rotenone. The role of ROS in the reaction also needs clarifying.

The reaction did not occur in the cytosolic fraction. This may suggest that the reaction is promoted in cells by mitochondria, with or without intervention of the ETC. On the other hand, it has been already demonstrated on this work that low-weight reducing biomolecules that are present in the cytosol are able to promote the reaction *in vitro*, so it is possible that the high dilution of the cytosol extract in the commercial cellular fractionation reagents prevents them to adequately promote the reaction in this case. Furthermore, the fractionation reagents could be inhibiting the reaction. To properly evaluate the reaction in a milieu that is representative of the cytosol, the cytosolic fraction should be isolated by mechanical means in a smaller volume. Alternatively, a cell-free

strategy could be employed to construct a cytosolic model with the adequate concentrations of low-weight biomolecules.

3.4.4. Experiments in *E. coli*

To test if the reaction could also be promoted by procaryotic cells, it was tried in the DH5 α strain of *E. coli*. The bacteria were incubated for 1 h at 37 °C with 100 μ M of the reactants in 1 mL PBS with 0.5% v/v of DMSO. Three treatments were tried: incubation with compound **2** to determine its internalization, with reactants **1** and **2** simultaneously, and with compound **2** followed by a wash with PBS and incubation with compound **1** for another hour (sequential treatment). These treatments were also replicated with a heat shock (HS) treatment by subjecting the cultures to 42 °C for 20 s immediately at the beginning of the first incubation. After incubation, cultures were centrifuged, and the culture media were retired. The remaining pellets were washed with PBS and centrifuged again. Culture media, washings and pellets were analyzed independently by HPLC-MS. Results are shown on Figure 3.

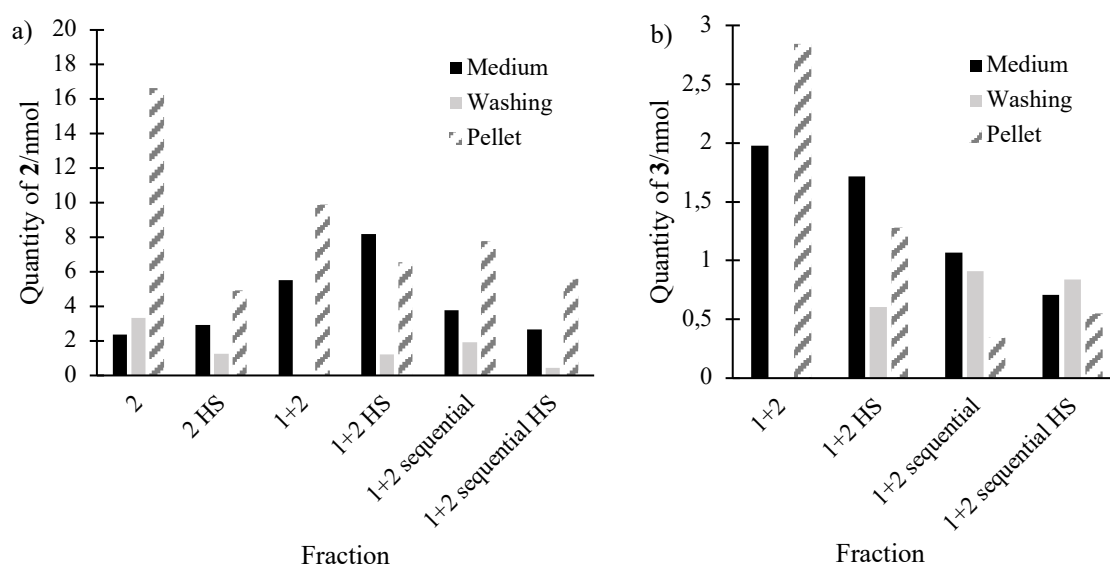


Figure 3. Quantification of compounds **2** (a) and **3** (b) in *E. coli* incubated with **1** and **2** simultaneously or sequentially. HS: heat shock (42 °C for 20 s). Washing fraction for **1+2** was lost in processing.

Again, these results are preliminary, and they should be considered qualitatively only until the experiments can be repeated several times to give reliable quantitative data. The extraction method clearly needs to be optimized, as only 10–20 nmol of **2** and **3** were recovered in total. It also seems that naphthoquinone **2** precipitates and accumulates in the pellet during centrifugation, so the concentration in the retired supernatant is very low

and the quantity of **2** calculated for the pellet is not representative of the cellular content. In contrast, in the experiment with HeLa cells twenty-five more times of **2** was recovered from the medium and washings than from the cellular extraction, but the procedure did not include any centrifugation step.

These results are insufficient to justify that the reaction proceeds intracellularly, as the presence of product **3** in the pellet could be also due to precipitation. On the other hand, the fact that **3** is recovered from the culture medium in comparable quantities is indicative that the reaction takes place extracellularly, at least partially. This agrees with previous studies, as Nothling *et al.*²⁸ already noted that the reducing milieu generated by *E. coli* in its culture medium can promote decomposition of arenediazonium compounds to give aryl radicals.

3.5. Experimental procedures

3.5.1. General information for in vitro experiments

Chemicals were acquired from Sigma Aldrich, Panreac, GE Healthcare, Alfa Aesar and Serva, and were used without further purification. The solvents used in reactions are of reagent grade unless otherwise noted. Dry solvents were purchased from Sigma Aldrich and used without further purification.

TLC was performed in 4x6 cm aluminum plates with silica gel Merck 60 F₂₅₄ and visualized under UV ($\lambda=254$ and 365 nm).

For irradiation experiments, a blue Kessil LED PhotoReaction Lighting PR160L-456 nm lamp was used.

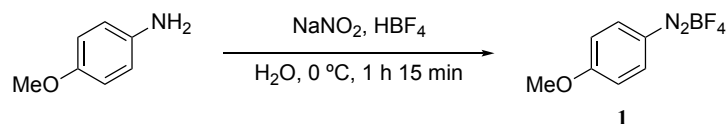
Vacuum concentration was achieved by rotary evaporation on a Büchi R-210 rotary evaporator, with a V-850 vacuum regulator, V-700 vacuum pump and B-491 thermostatic bath, followed by evaporation under high vacuum.

NMR spectra were recorded on a VARIAN Mercury-300 and an Agilent VNMRS-300 spectrometers. Spectra were analyzed using MestreNova® data processing software (www.mestrelab.com). Data are represented as follows: chemical shift (δ) in parts per million (ppm) downfield from tetramethylsilane, multiplicity (s = singlet, d = doublet, m = multiplet), coupling constants (J) in Hertz (Hz). Spectra were calibrated to the residual solvent peak, when possible (CDCl_3 $\delta = 7.260$ ppm. $\text{d}_6\text{-DMSO}$ $\delta = 2.500$ ppm).

Analytical HPLC was performed on an HPLC-MS Thermo Ultimate 3000 coupled to a Bruker AmaZon SL mass spectrometer, using electrospray ionization (ESI) and a flow rate of 0.35 mL/min at room temperature.

3.5.2. Synthesis of *p*-methoxyphenyldiazonium tetrafluoroborate (**1**)

Some diazonium salts are stable and can be isolated, as is the case of compound **1**. The synthesis was performed by the classical diazotization procedure.⁷⁵

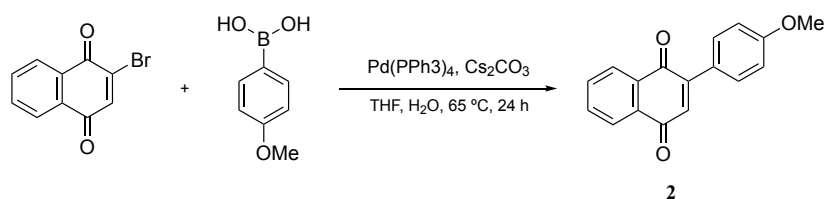


p-Anisidine (1.0 g, 8.12 mmol, 1 eq.) was suspended in 2.4 mL of water in a 25 mL round-bottom flask. Tetrafluoroboric acid (2.1 mL, 16.24 mmol, 2 eq.) was added to give a black solution. The reaction was cooled to 0 °C in a water-ice bath. A cold solution of sodium nitrite (1.12 g, 16.24 mmol, 2 eq.) in 2.4 mL of water was added dropwise. The mixture turned dark green, and the formation of a grey solid was observed. After 1 h 15 min, the solid was isolated by filtration as a grey powdery solid, washed with cold diethyl ether, redissolved in acetone, and recrystallized in diethyl ether to give pure **1** as a grey solid (1.2 g, 66%).

¹H-NMR (300 MHz, d₆-DMSO) δ 8.61 (d, *J* = 9.0 Hz, 2H), 7.48 (d, *J* = 9.0 Hz, 2H), 4.04 (s, 3H). Data in accordance with the literature.⁷⁶

3.5.3. Synthesis of 2-(4-methoxyphenyl)naphthalene-1,4-dione (**2**)

Procedure was adapted from literature.⁷⁷



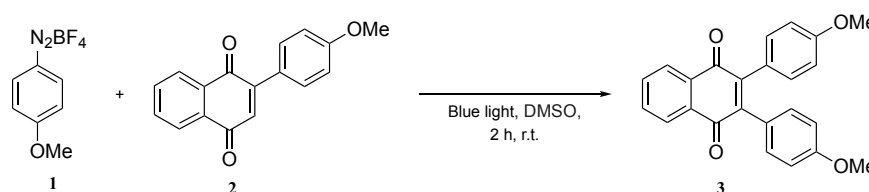
Tetrakis(triphenylphosphine)palladium(0) (28.9 mg, 0.025 mmol, 0.025 eq.) was dissolved in 4.0 mL of anhydrous THF in a purged Schlenk tube under nitrogen atmosphere. 2-Bromonaphthalene-1,4-dione (237.5 mg, 1.0 mmol, 1 eq.), cesium carbonate (488.7 mg, 1.5 mmol, 1.5 eq.) and 4-methoxyphenylboronic acid (227.9 mg, 1.5 mmol, 1.5 eq.) were successively added to the stirred solution under N₂ flow. Then, 0.6 mL of water were added. The mixture was heated to 65 °C until TLC (silica gel, *n*-hexane/ethyl acetate 9:1) showed complete consumption of the starting material (20 h). After cooling to ambient temperature, the mixture was diluted with water (15 mL) and

extracted three times with ethyl acetate. The combined organic layers were washed with brine, dried over MgSO_4 , and concentrated under vacuum. The product was purified by flash chromatography on silica gel (*n*-hexane/ethyl acetate, gradient from 0% to 20%) as an orange solid (238.4 mg, 90%), which turned red after dissolving in dichloromethane and concentrating under vacuum.

$^1\text{H-NMR}$ (300 MHz, *d*-chloroform) δ 8.21–8.08 (m, 2H), 7.79–7.78 (m, 2H), 7.59 (d, $J = 8.5$ Hz, 2H), 7.08–6.96 (m, 3H), 3.87 (s, 3H). $R_f = 0.33$ (*n*-hexane/ethyl acetate 9:1). Data in accordance with the literature.⁴⁴

3.5.4. Synthesis of 2,3-bis(4-methoxyphenyl)naphthalene-1,4-dione (**3**)

Compound **3** was synthesized for characterization following standard blue-light-promoted Meerwein arylation between compounds **1** and **2**.



Diazonium salt **1** (44.4 mg, 0.20 mmol, 1 eq.) and naphthoquinone **2** (158.6 mg, 0.6 mmol, 3 eq.) were introduced under nitrogen flow in a purged 50 mL Schlenk tube. The tube was then purged with three vacuum-nitrogen cycles. 20 mL of anhydrous DMSO was added to yield an orange solution. The solution was irradiated with a blue LED lamp (456 nm, 60 mW/cm², distance 10 cm). Bubbling was observed, and the solution turned dark red in 10 min. After 2 h, the solution was diluted with water (100 mL) and extracted three times with diethyl ether. The combined organic layers were washed with brine, dried over MgSO_4 , and concentrated under vacuum. The product was purified by flash chromatography on silica gel (*n*-hexane/ethyl acetate, gradient from 0% to 20%) as a red solid (28.4 mg, 38%).

$^1\text{H-NMR}$ (300 MHz, *d*-chloroform) δ 8.17 (d, $J = 4.0$ Hz, 2H), 7.76 (d, $J = 4.1$ Hz, 2H), 7.03 (d, $J = 8.3$ Hz, 4H), 6.78 (d, $J = 8.5$ Hz, 4H), 3.78 (s, 6H). $R_f = 0.22$ (*n*-hexane/ethyl acetate 9:1). Data in accordance with the literature.⁴⁴

3.5.5. Representative procedure for irradiation experiments in subsection 3.2

Diazonium salt **1** (2.2 mg, 0.01 mmol, 1 eq.), naphthoquinone **2** (7.9 mg, 0.03 mmol, 3 eq.) and $\text{Ru}(\text{bpy})_3$ (0.4 mg, 0.5 nmol, 0.05 eq.) were introduced under nitrogen flow in a purged 10 mL Schlenk tube. The tube was then purged with three vacuum-nitrogen cycles. 1 mL of anhydrous DMSO was added to yield an orange

solution. The solution was magnetically stirred and irradiated with a blue LED lamp (456 nm, 60 mW/cm², distance: 10 cm). Bubbling was observed, and the solution turned dark red in 10 min. After 2 h, the solution was diluted with water (5 mL) and extracted three times with diethyl ether. The combined organic layers were washed with brine, dried over MgSO₄, and concentrated under vacuum. A yield of 85% was determined by ¹H-NMR using dibromomethane as internal standard.

3.5.6. Representative procedure for reactions in subsection 3.3

Diazonium salt **1** (2.2 mg, 0.01 mmol, 1 eq.), naphthoquinone **2** (7.9 mg, 0.03 mmol, 3 eq.) and NADH disodium salt (7.1 mg, 0.01 mmol, 1 eq.) were introduced under nitrogen flow in a purged 10 mL Schlenk tube. The tube was then purged with three vacuum-nitrogen cycles. 1 mL of anhydrous DMSO was added to yield an orange solution. The solution was magnetically stirred. Bubbling was observed, and the solution turned dark red in 10 min. After 2 h, the solution was diluted with water (5 mL) and extracted three times with diethyl ether. The combined organic layers were washed with brine, dried over MgSO₄, and concentrated under vacuum. A yield of 77% was determined by ¹H-NMR using dibromomethane as internal standard.

3.5.7. Representative procedure for reactions in subsection 3.3.4

Diazonium salt **10** (5.4 mg, 0.02 mmol, 1 eq.) and NADH disodium salt (14.2 mg, 0.02 mmol, 1 eq.) were introduced under nitrogen flow in a purged 10 mL Schlenk tube. The tube was then purged with three vacuum-nitrogen cycles. Phenylacetylene (22.0 μL, 0.20 mmol, 10 eq.) was dissolved in 1 mL of anhydrous DMSO and added to the Schlenk to yield a yellow solution. The solution was magnetically stirred. Bubbling was observed, and the solution turned orange in 10 min. After 2 h, the solution was diluted with water (5 mL) and extracted three times with diethyl ether. The combined organic layers were washed with brine, dried over MgSO₄, and concentrated under vacuum. A yield of 43% was determined by ¹H-NMR using dibromomethane as internal standard.

3.5.8. Internal standard method for yield quantification

NMR has been established as a state-of-the-art method for determination of reaction yields from non-purified crudes, provided that the product presents one or more well-resolved signals. As the area under an NMR peak is usually proportional to the number of nuclei, calibrating with an adequate internal standard allows for precise quantification.⁷⁸

Initially, nitromethane was selected as internal standard for this project, but integration of signals for excess of compound **2** when following the studied reaction yielded inconsistent and usually excessive values. This was attributed to the high volatility of nitromethane. Dibromomethane in CDCl₃ ($\delta=4.95$ ppm, s) was finally selected as internal standard due to the proximity of its signal to that of the methoxy groups of product **3**. For validation of dibromomethane concentration, 1,3,5-trimethoxybenzene ($\delta=3.8$ ppm, s) was used as secondary internal standard, but its overlapping with a signal of product **3** prevented its use for direct yield determination on the reaction crudes.

For determining the yield of product **3**, the signals for the methoxy moiety ($\delta=3.78$ ppm, s, 3H) and two aromatic H from the naphthoquinone moiety ($\delta=6.78$ ppm, d, 2H) were used. When the yields calculated from the two signals differed in more than 7%, only the lower value was considered. The necessary volume of dibromomethane was added so that for a yield of 100% the relation between the internal standard signal and the methoxy group signal would be 1:1 (Equation 1).

$$\begin{aligned} \text{Volume}_{\text{CBr}_2\text{H}_2} &= \text{moles of } \mathbf{3} \times \frac{6 \text{ H/mol of } \mathbf{3}}{2 \text{ H/mol of CBr}_2\text{H}_2} \times \frac{MW_{\text{CBr}_2\text{H}_2}}{\text{Purity}_{\text{CBr}_2\text{H}_2} \times \rho_{\text{CBr}_2\text{H}_2}} \\ &= 0.010 \text{ mmol} \times 3 \times \frac{173.835 \text{ mg mmol}^{-1}}{0.99 \times 2.477 \text{ mg } \mu\text{L}^{-1}} = 2.13 \mu\text{L} \end{aligned}$$

Equation 1.

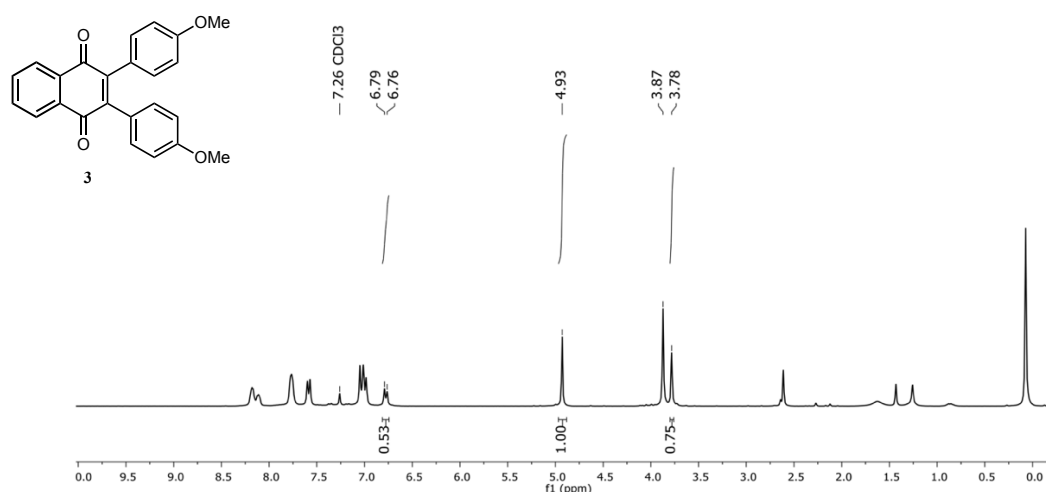


Figure 4. Example of yield determination by internal standard of dibromomethane (spectrum corresponding to procedure described in subsection 3.5.6).

For the compounds in subsections 3.3.3 and 3.3.4, the following peaks were employed for quantification based on literature reports: **7**: 3.86 (s, 3H),⁴⁴ 2.12 (s, 3H). **8**:

3.88 (s, 3H).⁴⁴ **9**: 3.86 (s, 3H).⁷⁹ **13**: 3.89 (s, 3H).⁶⁶ **14**: 4.05 (s, 3H).⁶⁷ **15**: 4.05 (s, 3H), 4.03 (s, 3H), 8.48 (s, 1H).⁶⁷

3.5.9. General information for cell culture experiments

HeLa and A549 cell cultures were incubated in DMEM (Dulbecco's modified Eagle's medium) from Sigma-Aldrich supplemented with 10% v/v fetal bovine serum (FBS), 1% penicillin/streptomycin and 1% L-glutamine from Thermo Fisher. Cultures were incubated at 37 °C, 5% CO₂ and 95% humidity. DMEM was purchased from Sigma-Aldrich. The other components were from Thermo Fisher. *E. coli* cultures were incubated in LB (lysogeny broth) composed of 10 g of Bacto Triptone from Gybco, 5 g of yeast extract from AppliChem and 10 g of NaCl from Sigma-Aldrich. Sterile PBS and DMSO of biological grade from Sigma-Aldrich were employed as solvents.

Luminescence was measured with an Infinite M Plex Tecan plate reader. Work was performed on a HR1200-IIA2 biological safety cabinet.

3.5.10. Luminescence viability assay

HeLa cells were seeded in a black wall 96-well plate with a confluence of 15 000 cells/well (1 day assay) or 1 000 cells/well (2 days assay, with starvation) and were incubated for 1 day in DMEM supplemented with 10% FBS (1 day assay), or 2 days changing the medium on the night of the second day with DMEM supplemented with 1% FBS (2 days assay). After that, the cells were treated with 100 µM of a suspension of compounds **1**, **2** or **3**, or **1** and **2** in DMEM with 0.5% v/v DMSO. After 1 h, the medium was changed for 100 µL of DMEM without phenol red and 100 µM of the commercial reagent from the CellTiter-Glo luminescent cell viability assay, and the luminescence signal was measured on a plate reader.

3.5.11. Experiment in HeLa cells

HeLa cells were incubated on four 100 mm Petri dish with a confluence of 6x10⁶ cells/dish with 3 mL of a suspension of compounds **1** and **2** (both 100 µM) in DMEM with 0.5% v/v of DMSO. After 1 h, the culture medium was collected and kept for posterior analysis. Cells were washed two times with 1 mL of PBS, which were collected separately for analysis. Cells were treated with 1 mL of Triton X-100 for lysing. All four fraction were lyophilized and dissolved in 1 mL of a 100 µM solution of coumarin in acetonitrile by vortex agitation and sonication for 15 min at 45 °C. The mixture was separated by centrifugation at 7 800 g for 10 min, and the supernatant was collected, filtered by HPLC filter, and analyzed by HPLC-MS.

3.5.12. Cell fragmentation assay

A549 cells were seeded in four 100 mm Petri dishes with a confluence of 700 000 cells/plate. Cells were washed with PBS, harvested with a scraper, and resuspended in 1 mL of PBS. 2x1 mL were separated into two 2 mL Eppendorf tubes ((a) for whole mitochondria experiments, and (b) for mitochondrial lysate experiments), and 250 μ L were separated to another tube for control with whole cells (c). The mitochondria isolation kit from cultured cells from Thermo Fisher (option A of the instructions) was employed to obtain a mitochondria-enriched fraction from tubes (a) and (b). 1.592 mL of one of the cytosolic fractions were kept for the experiment in cytosolic fraction (d). The mitochondrial fractions were resuspended in 1.592 mL of PBS. Mitochondria on tube (b) were sonicated with 2 pulses of 5 s.

All tubes were treated with 4 μ L of a 40 μ M suspension of compound **1** in DMSO and 4 μ L of a 40 μ M suspension of compound **2** in DMSO and incubated for 1 h at 37 °C with agitation. Tubes (a) and (c) were centrifugated at 12 300 g for 10 min and 1 700 g for 5 min, respectively. The supernatant was then retired, and the pellets were washed with PBS and centrifugated again in the same conditions. Liquid fractions were lyophilized for all tubes, and pellets obtained from (a) and (c) were dissolved in methanol and concentrated under vacuum. Each fraction from each tube was then dissolved in 1 mL of acetonitrile and sonicated for 15 min at 45 °C. The mixtures were centrifugated at 7 800g for 10 min, and the supernatant was collected, filtered with a HPLC filter, and analyzed by HPLC-MS.

3.5.13. Experiments in *E. coli*

A 10 mL preculture of DH5- α *E. coli* was diluted in 100 mL of LB and incubated at 37 °C with stirring until reaching an OD of 0.3. Six 10 mL aliquots of the culture were centrifugated at 3 000 g for 15 min. For normal treatment (a, b, c) the isolated pellet was resuspended in 1 mL of a solution 100 μ M of compound **2** (a, c) or 100 μ M of compounds **1** and 100 μ M of **2** (b), in PBS with DMSO 0.5% v/v and incubated at 37 °C for 2 h with stirring. The tubes were centrifugated at 3 000 g for 15 min, and the supernatant was collected. The pellets were washed with 1 mL of PBS, centrifugated at 3 000 g for 10 min, and the supernatant was again collected. 1 mL of a 100 μ M solution of compound **1** in PBS with 0.5% v/v DMSO was added to tube (c) and incubated with stirring at 37 °C for 1 h. Tube (c) was then centrifugated at 3 000 g for 10 min, and the supernatant was collected. For heat shock treatment (d, e, f), the first incubation was substituted by heat

shock (41 °C for 20 s) followed by ice incubation for 30 min and stirred incubation at 37 °C for 30 min.

Liquid fractions were lyophilized. All fractions and pellets were dissolved in 1 mL of a 100 µM solution of coumarin in acetonitrile and sonicated for 15 min at 45 °C. The mixtures were centrifugated at 7 800g for 10 min, and the supernatant was collected, filtered with a HPLC filter, and analyzed by HPLC-MS.

3.5.14. Quantification by HPLC-MS

Concentration of **1** and **2** was determined from the areas under the absorbance peak at 270 nm in HPLC. Coumarin was used as internal standard. The calibration lines employed were $y=0,09326332x+0,02085394$ ($R^2=0,9984$) for compound **2** and $y=0,06245542x-0,000925$ ($R^2=0,9997$) for product **3**, being y the quotient of the area under the peak for the compound and coumarin, and x the concentration of the compound in µM. The calibration curves were constructed and generously shared by member of the group.

4. Conclusions

In this Degree Final Project, a new biocompatible reaction promoted intracellularly by mammal cells (HeLa and A549) based on a Meerwein arylation of a naphthoquinone is described. The reaction was also found to take place in presence of *E. coli*. The reaction is promoted in abiotic environments by low-weight biological reductants NADH, glutathione and ascorbate, and experimental results suggest that the NADH-promoted reaction begins with a single electron transfer from NADH to the diazonium salt to give a radical, and then proceeds by a radical chain mechanism. The reaction was found to occur in isolated mitochondria and in mitochondria lysate, although additional research is needed to clarify the mechanism by which the reaction is promoted in cells. Finally, preliminary studies in abiotic media showed that NADH can promote synthesis of benzothiophenes and phenanthrenes from diazonium salts and alkynes in abiotic media.

These findings would enable the development of cell-promoted biocompatible reactions based on diazonium compounds with applications in biosynthesis and biomedicine. The study of these transformations in alternative cell types could be of great interest, as diazonium salts may be engineered to react selectively in highly reductive milieus, such as those present in some tumor microenvironments. This would allow for localized *in situ* synthesis of probes and drugs.

Conclusiones

En este Trabajo de Fin de Grado, se ha descrito una nueva reacción biocompatible promovida intracelularmente por células de mamífero (HeLa y A549) basada en la arilación de Meerwein de una naftoquinona. Se encontró que la reacción también tiene lugar en presencia de *E. coli*. En ambientes abióticos, promueven la reacción reductores biológicos de bajo peso molecular como el NADH, el glutatión y el ascorbato, y los resultados experimentales sugieren que la reacción promovida por el NADH comienza con una transferencia de un electrón del NADH a la sal de diazonio para dar un radical, y a continuación procede por un mecanismo radicalario en cadena. Se vio que la reacción transcurre en mitocondrias aisladas, aunque se requieren estudios adicionales para aclarar el mecanismo por el que las células promueven la reacción. Finalmente, se llevaron a cabo estudios preliminares que muestran que el NADH puede promover la síntesis de benzotiofenos y fenantrenos a partir de sales de diazonio y alquinos en medios abióticos.

Estos resultados podrían permitir el desarrollo de reacciones biocompatibles promovidas por la célula basadas en compuestos de diazonio con aplicaciones en biosíntesis y biomedicina. El estudio de estas transformaciones en tipos celulares alternativos es de gran interés, ya que podrían diseñarse sales de diazonio que reaccionasen selectivamente en ambientes altamente reductores, como los que se encuentran en algunos microambientes tumorales. Ello permitiría la síntesis *in situ* localizada de sondas y fármacos.

Conclusión

Neste Traballo de Fin de Grao, describiuse unha nova reacción biocompatible promovida intracelularmente por células de mamífero (HeLa e A549) baseada nunha arilación de Meerwein dunha naftoquinona. Atopouse que a reacción tamén ten lugar en presenza de *E. coli*. En ambientes abióticos, promoven a reacción reductores biolóxicos de baixo peso molecular coma o NADH, o glutatión e o ascorbato, e os resultados experimentais suxiren que a reacción promovida polo NADH comeza cunha transferencia dun electrón do NADH ao sal de diazonio para dar un radical, e a continuación procede por un mecanismo radicalario en cadea. Atopouse que a reacción transcorre en mitocondrias illadas, aínda que se requiren estudos adicionais para aclarar o mecanismo polo que as células promoven a reacción. Finalmente, leváronse a cabo estudos

preliminares que mostran que o NADH pode promover a síntese de benzotiofenos e fenantrenos a partir de sales de diazonio e alquinos en medios abióticos.

Estes resultados poderían permitir o desenvolvemento de reaccións biocompatibles promovidas pola célula baseadas en compostos de diazonio con aplicacións en biosíntese e biomedicina. O estudo desta transformación en tipos celulares alternativos é de gran interese, xa que poderían deseñarse sales de diazonio que reaccionasen selectivamente en ambientes altamente redutores, coma os que se atopan nalgúns microambientes tumorais. Elo permitiría a síntese *in situ* localizada de sondas e fármacos.

References

- (1) Sletten, E. M.; Bertozzi, C. R. Bioorthogonal Chemistry: Fishing for Selectivity in a Sea of Functionality. *Angew Chem Int Ed* **2009**, *48* (38), 6974–6998. <https://doi.org/10.1002/anie.200900942>.
- (2) Hang, H. C.; Yu, C.; Kato, D. L.; Bertozzi, C. R.; Simons, K. A Metabolic Labeling Approach toward Proteomic Analysis of Mucin-Type O-Linked Glycosylation. *Proc Natl Acad Sci U.S.A.* **2003**, *100* (25), 14846–14851. <https://doi.org/10.1073/pnas.2335201100>.
- (3) Wang, W.; Zhang, X.; Huang, R.; Hirschbiegel, C. M.; Wang, H.; Ding, Y.; Rotello, V. M. In Situ Activation of Therapeutics through Bioorthogonal Catalysis. *Adv Drug Deliv Rev* **2021**, *176*. <https://doi.org/10.1016/j.addr.2021.113893>.
- (4) Ramström, O. *Scientific Background on the Nobel Prize in Chemistry 2022 - Click Chemistry and Bioorthogonal Chemistry*; 2022. <https://www.nobelprize.org/uploads/2022/10/advanced-chemistryprize2022-2.pdf>.
- (5) Scinto, S. L.; Bilodeau, D. A.; Hincapie, R.; Lee, W.; Nguyen, S. S.; Xu, M.; am Ende, C. W.; Finn, M. G.; Lang, K.; Lin, Q.; Pezacki, J. P.; Prescher, J. A.; Robillard, M. S.; Fox, J. M. Bioorthogonal Chemistry. *Nat Rev Methods Primers* **2021**, *1*. <https://doi.org/10.1038/s43586-021-00028-z>.
- (6) Lim, R. K. V.; Lin, Q. Bioorthogonal Chemistry: Recent Progress and Future Directions. *Chem Commun* **2010**, *46* (10), 1589–1600. <https://doi.org/10.1039/b925931g>.
- (7) Lang, K.; Chin, J. W. Bioorthogonal Reactions for Labeling Proteins. *ACS Chem Biol* **2014**, *9* (1), 16–20. <https://doi.org/10.1021/cb4009292>.

- (8) Saxon, E.; Bertozzi, C. R. Cell Surface Engineering by a Modified Staudinger Reaction. *Science* **2000**, *287* (5460), 2007–2010. <https://doi.org/10.1126/science.287.5460.2007>.
- (9) Wang, Q.; Chan, T. R.; Hilgraf, R.; Fokin, V. V.; Sharpless, K. B.; Finn, M. G. Bioconjugation by Copper(I)-Catalyzed Azide-Alkyne [3 + 2] Cycloaddition. *J Am Chem Soc* **2003**, *125* (11), 3192–3193. <https://doi.org/10.1021/ja021381e>.
- (10) Yusop, R. M.; Unciti-Broceta, A.; Johansson, E. M. V.; Sánchez-Martín, R. M.; Bradley, M. Palladium-Mediated Intracellular Chemistry. *Nat Chem* **2011**, *3* (3), 239–243. <https://doi.org/10.1038/nchem.981>.
- (11) Li, N.; Lim, R. K. V.; Edwardraja, S.; Lin, Q. Copper-Free Sonogashira Cross-Coupling for Functionalization of Alkyne-Encoded Proteins in Aqueous Medium and in Bacterial Cells. *J Am Chem Soc* **2011**, *133* (39), 15316–15319. <https://doi.org/10.1021/ja2066913>.
- (12) Jeschek, M.; Reuter, R.; Heinisch, T.; Trindler, C.; Klehr, J.; Panke, S.; Ward, T. R. Directed Evolution of Artificial Metalloenzymes for in Vivo Metathesis. *Nature* **2016**, *537* (7622), 661–665. <https://doi.org/10.1038/nature19114>.
- (13) Ai, H.; Lee, J. W.; Schultz, P. G. A Method to Site-Specifically Introduce Methyllysine into Proteins in E. Coli. *Chem Commun* **2010**, *46* (30), 5506. <https://doi.org/10.1039/c0cc00108b>.
- (14) Sánchez, M. I.; Penas, C.; Vázquez, M. E.; Mascareñas, J. L. Metal-Catalyzed Uncaging of DNA-Binding Agents in Living Cells. *Chem Sci* **2014**, *5* (5), 1901–1907. <https://doi.org/10.1039/C3SC53317D>.
- (15) Miller, M. A.; Askevold, B.; Mikula, H.; Kohler, R. H.; Pirovich, D.; Weissleder, R. Nano-Palladium Is a Cellular Catalyst for in Vivo Chemistry. *Nat Commun* **2017**, *8* (1), 15906. <https://doi.org/10.1038/ncomms15906>.
- (16) Li, J.; Yu, J.; Zhao, J.; Wang, J.; Zheng, S.; Lin, S.; Chen, L.; Yang, M.; Jia, S.; Zhang, X.; Chen, P. R. Palladium-Triggered Deprotection Chemistry for Protein Activation in Living Cells. *Nat Chem* **2014**, *6* (4), 352–361. <https://doi.org/10.1038/nchem.1887>.
- (17) Dommerholt, J.; Schmidt, S.; Temming, R.; Hendriks, L. J. A.; Rutjes, F. P. J. T.; van Hest, J. C. M.; Lefeber, D. J.; Friedl, P.; van Delft, F. L. Readily Accessible Bicyclononynes for Bioorthogonal Labeling and Three-Dimensional Imaging of Living Cells. *Angew Chem Int Ed* **2010**, *49* (49), 9422–9425. <https://doi.org/10.1002/anie.201003761>.

- (18) Rossin, R.; Renart Verkerk, P.; van den Bosch, S. M.; Vulders, R. C. M.; Verel, I.; Lub, J.; Robillard, M. S. In Vivo Chemistry for Pretargeted Tumor Imaging in Live Mice. *Angew Chem Int Ed* **2010**, *49* (19), 3375–3378. <https://doi.org/10.1002/anie.200906294>.
- (19) Wallace, S.; Balskus, E. P. Opportunities for Merging Chemical and Biological Synthesis. *Curr Opin Biotechnol* **2014**, *30*, 1–8. <https://doi.org/10.1016/j.copbio.2014.03.006>.
- (20) Sadler, J. C.; Dennis, J. A.; Johnson, N. W.; Wallace, S. Interfacing Non-Enzymatic Catalysis with Living Microorganisms. *RSC Chem. Biol* **2021**, *2*, 1073–1083. <https://doi.org/10.1039/d1cb00072a>.
- (21) Wu, J.; Lin, J.; Huang, P. Harnessing Abiotic Organic Chemistry in Living Systems for Biomedical Applications. *Chem Soc Rev* **2023**. <https://doi.org/10.1039/D3CS00280B>.
- (22) Go, Y.-M.; Jones, D. P. Redox Compartmentalization in Eukaryotic Cells. *Biochim Biophys Acta Gen Subj* **2008**, *1780* (11), 1273–1290. <https://doi.org/10.1016/j.bbagen.2008.01.011>.
- (23) Hernandez, M. E.; Newman, D. K. Extracellular Electron Transfer. *CMLS, Cell. Mol. Life Sci* **2001**, *58*, 1562–1571. <https://doi.org/10.1007/PL00000796>.
- (24) Dai, Y.; Li, T.; Zhang, Z.; Tan, Y.; Pan, S.; Zhang, L.; Xu, H. Oxidative Polymerization in Living Cells. *J Am Chem Soc* **2021**, *143* (28), 10709–10717. <https://doi.org/10.1021/jacs.1c04821>.
- (25) Shen, Q.; Huang, Y.; Zeng, Y.; Zhang, E.; Lv, F.; Liu, L.; Wang, S. Intracellular Radical Polymerization of Paclitaxel-Bearing Acrylamide for Self-Inflicted Apoptosis of Cancer Cells. *ACS Mater Lett* **2021**, *3* (9), 1307–1314. <https://doi.org/10.1021/acsmaterialslett.1c00357>.
- (26) Magennis, E. P.; Fernandez-Trillo, F.; Sui, C.; Spain, S. G.; Bradshaw, D. J.; Churchley, D.; Mantovani, G.; Winzer, K.; Alexander, C. Bacteria-Instructed Synthesis of Polymers for Self-Selective Microbial Binding and Labelling. *Nat Mater* **2014**, *13* (7), 748–755. <https://doi.org/10.1038/nmat3949>.
- (27) Fan, G.; Dundas, C. M.; Graham, A. J.; Lynd, N. A.; Keitz, B. K. *Shewanella Oneidensis* as a Living Electrode for Controlled Radical Polymerization. *Proc Natl Acad Sci U.S.A.* **2018**, *115* (18), 4559–4564. <https://doi.org/10.1073/pnas.1800869115>.

- (28) D. Nothling, M.; Cao, H.; G. McKenzie, T.; M. Hocking, D.; A. Strugnell, R.; G. Qiao, G. Bacterial Redox Potential Powers Controlled Radical Polymerization. *J Am Chem Soc* **2021**, *143* (1), 286–293. <https://doi.org/10.1021/jacs.0c10673>.
- (29) Gamcsik, M. P.; Kasibhatla, M. S.; Teeter, S. D.; Colvin, O. M. Glutathione Levels in Human Tumors. *Biomarkers* **2012**, *17* (8), 671–691. <https://doi.org/10.3109/1354750X.2012.715672>.
- (30) Kalinina, E. V.; Gavriliuk, L. A. Glutathione Synthesis in Cancer Cells. *Biochem (Mosc)* **2020**, *85* (8), 895–907. <https://doi.org/10.1134/S0006297920080052>.
- (31) Liang, G.; Ren, H.; Rao, J. A Biocompatible Condensation Reaction for Controlled Assembly of Nanostructures in Living Cells. *Nat Chem* **2010**, *2* (1), 54–60. <https://doi.org/10.1038/nchem.480>.
- (32) Cui, L.; Vivona, S.; Smith, B. R.; Kothapalli, S.-R.; Liu, J.; Ma, X.; Chen, Z.; Taylor, M.; Kierstead, P. H.; Fréchet, J. M. J.; Gambhir, S. S.; Rao, J. Reduction Triggered in Situ Polymerization in Living Mice. *J Am Chem Soc* **2020**, *142* (36), 15575–15584. <https://doi.org/10.1021/jacs.0c07594>.
- (33) Heng, H.; Song, G.; Cai, X.; Sun, J.; Du, K.; Zhang, X.; Wang, X.; Feng, F.; Wang, S. Intrinsic Mitochondrial Reactive Oxygen Species (ROS) Activate the In Situ Synthesis of Trimethine Cyanines in Cancer Cells. *Angew Chem Int Ed* **2022**, *61* (38), e202203444. <https://doi.org/10.1002/anie.202203444>.
- (34) Zhao, C.; Li, Z.; Chen, J.; Su, L.; Wang, J.; Chen, D. S.; Ye, J.; Liao, N.; Yang, H.; Song, J.; Shi, J. Site-specific Biomimicry of Antioxidative Melanin Formation and Its Application for Acute Liver Injury Therapy and Imaging. *Adv Mater* **2021**, *33* (34), 2102391. <https://doi.org/10.1002/adma.202102391>.
- (35) Liu, J.; Chan, S. H. J.; Brock-Nannestad, T.; Chen, J.; Lee, S. Y.; Solem, C.; Jensen, P. R. Combining Metabolic Engineering and Biocompatible Chemistry for High-Yield Production of Homo-Diacetyl and Homo-(S,S)-2,3-Butanediol. *Metab Eng* **2016**, *36*, 57–67. <https://doi.org/10.1016/j.ymben.2016.02.008>.
- (36) Prasad Hari, D.; König, B. The Photocatalyzed Meerwein Arylation: Classic Reaction of Aryl Diazonium Salts in a New Light. *Angew Chem Int Ed* **2013**, *52*, 4734–4743. <https://doi.org/10.1002/anie.201210276>.
- (37) Babu, S. S.; Muthuraja, P.; Yadav, P.; Gopinath, P. Aryldiazonium Salts in Photoredox Catalysis – Recent Trends. *Adv Synth Catal* **2021**, *363* (7), 1782–1809. <https://doi.org/10.1002/adsc.202100136>.

- (38) Wang, M.; Tang, B.-C.; Xiang, J.-C.; Chen, X.-L.; Ma, J.-T.; Wu, Y.-D.; Wu, A.-X. Aryldiazonium Salts Serve as a Dual Synthon: Construction of Fully Substituted Pyrazoles via Rongalite-Mediated Three-Component Radical Annulation Reaction. *Org Lett* **2019**, *21* (22), 8934–8937. <https://doi.org/10.1021/acs.orglett.9b03212>.
- (39) Vollhardt, P.; Schore, N. *Organic Chemistry. Structure and Function*, 7th ed.; Fiorillo, J., Ed.; W.H. Freeman and Company: New York, 2014.
- (40) Galli, C. Radical Reactions of Arenediazonium Ions: An Easy Entry into the Chemistry of the Aryl Radical. *Chem Rev* **1988**, *88* (5), 765–792. <https://doi.org/10.1021/cr00087a004>.
- (41) Milanesi, S.; Fagnoni, M.; Albin, A. (Sensitized) Photolysis of Diazonium Salts as a Mild General Method for the Generation of Aryl Cations. Chemoselectivity of the Singlet and Triplet 4-Substituted Phenyl Cations. *J Org Chem* **2005**, *70* (2), 603–610. <https://doi.org/10.1021/jo048413w>.
- (42) Scarpa de Souza, E. L.; Oliveira, C. C. Selective Radical Transformations with Aryldiazonium Salts. *Eur J Org Chem*. John Wiley and Sons Inc March 21, 2023, pp 105–127. <https://doi.org/10.1002/ejoc.202300073>.
- (43) Schroll, P.; Hari, D. P.; König, B. Photocatalytic Arylation of Alkenes, Alkynes and Enones with Diazonium Salts. *ChemistryOpen* **2012**, *1* (3), 130–133. <https://doi.org/10.1002/open.201200011>.
- (44) Nagar, B.; Dhar, B. B. Photochemical C–H Arylation of Naphthoquinones Using Eosin Y. *ACS Omega* **2022**, *7* (36), 32615–32619. <https://doi.org/10.1021/acsomega.2c04289>.
- (45) Witzel, S.; Hoffmann, M.; Rudolph, M.; Kerscher, M.; Comba, P.; Dreuw, A.; Hashmi, A. S. K. Excitation of Aryl Cations as the Key to Catalyst-Free Radical Arylations. *Cell Rep Phys Sci* **2021**, *2*. <https://doi.org/10.1016/j.xcrp.2021.100325>.
- (46) Wang, D.; Cheng, C.; Wu, Q.; Wang, J.; Kang, Z.; Guo, X.; Wu, H.; Hao, E.; Jiao, L. Visible-Light Excitation of BODIPYs Enables Self-Promoted Radical Arylation at Their 3,5-Positions with Diazonium Salts. *Org Lett* **2019**, *21* (13), 5121–5125. <https://doi.org/10.1021/acs.orglett.9b01722>.
- (47) Reszka, K. J.; Chignell, C. F. One-Electron Reduction of Arenediazonium Compounds by Physiological Electron Donors Generates Aryl Radicals. An EPR and Spin Trapping Investigation. *Chem Biol Interact* **1995**, *96* (3), 223–234. [https://doi.org/10.1016/0009-2797\(94\)03593-W](https://doi.org/10.1016/0009-2797(94)03593-W).

- (48) Forman, H. J.; Zhang, H.; Rinna, A. Glutathione: Overview of Its Protective Roles, Measurement, and Biosynthesis. *Mol Aspects Med* **2009**, *30* (1–2), 1–12. <https://doi.org/10.1016/j.mam.2008.08.006>.
- (49) Meister, A. Glutathione Metabolism and Its Selective Modification. *J Biol Chem* **1988**, *263* (33), 17205–17208.
- (50) Yamada, K.; Hara, N.; Shibata, T.; Osago, H.; Tsuchiya, M. The Simultaneous Measurement of Nicotinamide Adenine Dinucleotide and Related Compounds by Liquid Chromatography/Electrospray Ionization Tandem Mass Spectrometry. *Anal Biochem* **2006**, *352* (2), 282–285. <https://doi.org/10.1016/j.ab.2006.02.017>.
- (51) Yang, H.; Yang, T.; Baur, J. A.; Perez, E.; Matsui, T.; Carmona, J. J.; Lamming, D. W.; Souza-Pinto, N. C.; Bohr, V. A.; Rosenzweig, A.; de Cabo, R.; Sauve, A. A.; Sinclair, D. A. Nutrient-Sensitive Mitochondrial NAD⁺ Levels Dictate Cell Survival. *Cell* **2007**, *130* (6), 1095–1107. <https://doi.org/10.1016/j.cell.2007.07.035>.
- (52) Swierczyński, J.; Słomińska, E.; Smoleński, R. T.; Mayer, D. Increase in NAD but Not ATP and GTP Concentrations in Rat Liver by Dehydroepiandrosterone Feeding. *Pol J Pharmacol* **2001**, *53* (2), 125–130.
- (53) Sallin, O.; Reymond, L.; Gondrand, C.; Raith, F.; Koch, B.; Johnsson, K. Semisynthetic Biosensors for Mapping Cellular Concentrations of Nicotinamide Adenine Dinucleotides. *Elife* **2018**, *7*. <https://doi.org/10.7554/eLife.32638>.
- (54) Williamson, D.; Lund, P.; Krebs, H. The Redox State of Free Nicotinamide-Adenine Dinucleotide in the Cytoplasm and Mitochondria of Rat Liver. *Biochem J* **1967**, *103* (2), 514–527. <https://doi.org/10.1042/bj1030514>.
- (55) Zhang, Q.; Piston, D. W.; Goodman, R. H. Regulation of Corepressor Function by Nuclear NADH. *Science* **2002**, *295* (5561), 1895–1897. <https://doi.org/10.1126/science.1069300>.
- (56) Yang, H.; Yang, T.; Baur, J. A.; Perez, E.; Matsui, T.; Carmona, J. J.; Lamming, D. W.; Souza-Pinto, N. C.; Bohr, V. A.; Rosenzweig, A.; de Cabo, R.; Sauve, A. A.; Sinclair, D. A. Nutrient-Sensitive Mitochondrial NAD⁺ Levels Dictate Cell Survival. *Cell* **2007**, *130* (6), 1095–1107. <https://doi.org/10.1016/j.cell.2007.07.035>.
- (57) Zhitkovich, A. Ascorbate: Antioxidant and Biochemical Activities and Their Importance for in Vitro Models. *Arch Toxicol* **2021**, *95* (12), 3623–3631. <https://doi.org/10.1007/s00204-021-03167-0>.

- (58) Fukuzumi, S.; Suenobu, T.; Patz, M.; Hirasaka, T.; Itoh, S.; Fujitsuka, M.; Ito, O. Selective One-Electron and Two-Electron Reduction of C₆₀ with NADH and NAD Dimer Analogues via Photoinduced Electron Transfer. *J Am Chem Soc* **1998**, *120* (32), 8060–8068. <https://doi.org/10.1021/ja9813459>.
- (59) Yasui, S.; Nakamura, K.; Ohno, A. Reduction by a Model of NAD(P)H. 45. Mechanism for the Dediazonation of Arenediazonium Salts Initiated by One-Electron Transfer from an NAD(P)H Model. *J Org Chem* **1984**, *49* (5), 878–882. <https://doi.org/10.1021/jo00179a024>.
- (60) Archipowa, N.; Kutta, R. J.; Heyes, D. J.; Scrutton, N. S. Stepwise Hydride Transfer in a Biological System: Insights into the Reaction Mechanism of the Light-Dependent Protochlorophyllide Oxidoreductase. *Angew Chem Int Ed* **2018**, *57*, 2682–2686. <https://doi.org/10.1002/ange.201712729>.
- (61) Grodkowski, J.; Neta, P.; Carlson, B. W.; Miller, L. One-Electron Transfer Reactions of the Couple NAD./NADH. *J Phys Chem* **1983**, *87* (16), 3135–3138. <https://doi.org/10.1021/j100239a035>.
- (62) Zhu, X. Q.; Mu, Y. Y.; Li, X. T. What Are the Differences between Ascorbic Acid and NADH as Hydride and Electron Sources in Vivo on Thermodynamics, Kinetics, and Mechanism? *J Phys Chem B* **2011**, *115* (49), 14794–14811. <https://doi.org/10.1021/jp2067974>.
- (63) Tatumashvili, E.; Chan, B.; Nashar, P. E.; McErlean, C. S. P. σ -Bond Initiated Generation of Aryl Radicals from Aryl Diazonium Salts. *Org Biomol Chem* **2020**, *18* (9), 1812–1819. <https://doi.org/10.1039/D0OB00205D>.
- (64) Richter, D.; Mayr, H. Hydride-Donor Abilities of 1,4-Dihydropyridines: A Comparison with π Nucleophiles and Borohydride Anions. *Angew Chem Int Ed* **2009**, *48* (11), 1958–1961. <https://doi.org/10.1002/anie.200804263>.
- (65) Pramanik, M. M. D.; Rastogi, N. Visible Light Catalyzed Methylsulfoxidation of (Het)Aryl Diazonium Salts Using DMSO. *Chem Commun* **2016**, *52* (55), 8557–8560. <https://doi.org/10.1039/C6CC04142F>.
- (66) Hari, D. P.; Hering, T.; König, B. Visible Light Photocatalytic Synthesis of Benzothiophenes. *Org Lett* **2012**, *14* (20), 5334–5337. <https://doi.org/10.1021/ol302517n>.
- (67) Xiao, T.; Dong, X.; Tang, Y.; Zhou, L. Phenanthrene Synthesis by Eosin Y-Catalyzed, Visible Light-Induced [4+2] Benzannulation of Biaryldiazonium Salts

- with Alkynes. *Adv Synth Catal* **2012**, *354* (17), 3195–3199. <https://doi.org/10.1002/adsc.201200569>.
- (68) Niles, A. L.; Moravec, R. A.; Worzella, T. J.; Evans, N. J.; Riss, T. L. High-Throughput Screening Assays for the Assessment of Cytotoxicity. In *High-Throughput Screening Methods in Toxicity Testing*; Steinberg, P., Ed.; John Wiley & Sons, Inc.: Hoboken, NJ, USA, 2013; pp 107–127. <https://doi.org/10.1002/9781118538203.ch5>.
- (69) Forman, S.; Kas, J.; Fini, F.; Steinberg, M.; Ruml, T. The Effect of Different Solvents on the ATP/ADP Content and Growth Properties of HeLa Cells. *J Biochem Mol Toxicol* **1999**, *13* (1), 11–15. [https://doi.org/10.1002/\(SICI\)1099-0461\(1999\)13:1<11::AID-JBT2>3.0.CO;2-R](https://doi.org/10.1002/(SICI)1099-0461(1999)13:1<11::AID-JBT2>3.0.CO;2-R).
- (70) Davis, P. K.; Ho, A.; Dowdy, S. F. Biological Methods for Cell-Cycle Synchronization of Mammalian Cells. *Biotechniques* **2001**, *30* (6), 1322–1331. <https://doi.org/10.2144/01306rv01>.
- (71) Satoh, T.; Sakai, N.; Enokido, Y.; Uchiyama, Y.; Hatanaka, H. Survival Factor-Insensitive Generation of Reactive Oxygen Species Induced by Serum Deprivation in Neuronal Cells. *Brain Res* **1996**, *733* (1), 9–14. [https://doi.org/10.1016/0006-8993\(96\)00527-6](https://doi.org/10.1016/0006-8993(96)00527-6).
- (72) Alberts, B.; Johnson, A.; Lewis, J.; Raff, M.; Roberts, K.; Walter, P. The Compartmentalization of Cells. In *Molecular Biology of the Cell*; Garland Science: New York, 2002.
- (73) Kang, J.; Pervaiz, S. Mitochondria: Redox Metabolism and Dysfunction. *Biochem Res Int* **2012**, *2012*, 896751. <https://doi.org/10.1155/2012/896751>.
- (74) Alberts, B.; Johnson, A.; Lewis, J.; Raff, M.; Roberts, K.; Walter, P. Fractionation of Cells. In *Molecular Biology of the Cell*; Garland Science: New York, 2002.
- (75) Bonin, H.; Fouquet, E.; Felpin, F.-X. Aryl Diazonium versus Iodonium Salts: Preparation, Applications and Mechanisms for the Suzuki-Miyaura Cross-Coupling Reaction. *Adv Synth Catal* **2011**, *353* (17), 3063–3084. <https://doi.org/10.1002/adsc.201100531>.
- (76) Govaerts, S.; Nakamura, K.; Constantin, T.; Leonori, D. A Halogen-Atom Transfer (XAT)-Based Approach to Indole Synthesis Using Aryl Diazonium Salts and Alkyl Iodides. *Org Lett* **2022**, *24* (43), 7883–7887. <https://doi.org/10.1021/acs.orglett.2c02840>.

- (77) Zhang, H.; Wang, B.; Xu, H.; Li, F.-Y.; Wang, J.-Y. Synthesis of Naphthodihydrofurans via an Iron(III)-Catalyzed Reduction Radical Cascade Reaction. *Org Chem Front* **2021**, *8* (21), 6019–6025. <https://doi.org/10.1039/D1QO01041G>.
- (78) Rizzo, V.; Pinciroli, V. Quantitative NMR in Synthetic and Combinatorial Chemistry. *J Pharm Biomed Anal* **2005**, *38* (5), 851–857. <https://doi.org/10.1016/j.jpba.2005.01.045>.
- (79) Yu, D.; Chen, X.-L.; Ai, B.-R.; Zhang, X.-M.; Wang, J.-Y. Tetrabutylammonium Iodide Catalyzed Hydroxylation of Naphthoquinone Derivatives with Tert-Butyl Hydroperoxide as an Oxidant. *Tetrahedron Lett* **2018**, *59* (40), 3620–3623. <https://doi.org/10.1016/j.tetlet.2018.08.052>.

Figures created with ChemDraw and Biorender (www.biorender.com)

Annex: NMR spectra

